Imperial College London

Master Dissertation

Holographic Principle and Applications to Fermion Systems

Author:
Napat Poovuttikul

Supervisor:
Dr. Toby Wiseman

A dissertation submitted in fulfilment of the requirements for the degree of Master of Sciences

in the

Theoretical Physics Group
Imperial College London

September 2013

You need a different way of looking at them than starting from single particle descriptions. You don't try to explain the ocean in terms of individual water molecules

Sean Hartnoll [1]

Acknowledgements

I am most grateful to my supervisor, Toby Wiseman, who dedicated his time reading through my dissertation plan, answering a lot of tedious questions and give me number of insightful explanations. I would also like to thanks my soon to be PhD supervisor, Jan Zaanen, for sharing an early draft of his review in this topic and give me the opportunity to work in the area of this dissertation. I cannot forget to show my gratitude to Amihay Hanay for his exotic string theory course and Michela Petrini for giving very good introductory lectures in AdS/CFT.

I would particularly like to thanks a number of friends who help me during the period of the dissertation. I had valuable discussions with Simon Nakach, Christiana Pentelidou, Alex Adam, Piyabut Burikham, Kritaphat Songsriin. I would also like to thanks Freddy Page and Anne-Silvie Deutsch for their advices in using Inkscape, Matthew Citron, Christiana Pantelidou and Supakchi Ponglertsakul for their helps on Mathematica coding and typesetting latex. The detailed comments provided by Toby Wiseman and Simon Nakach were especially invaluable.

Contents

Chapter 1

Holographic and Condensed Matter Preliminary

1.1 Introduction : The duality

The duality is the far reaching theoretical physics concept, ranging from the quantum Hall fluid to string theory. It is often made out by some theorist to be a branch of higher mathematics but in fact it derives from an entirely physical idea. The two theories are said to be **dual** once there exist a set of dictionary rules that we can map one theory to the other. It is one of the key concept that leads to the revolution in string theory when people realise that six different string theories can be linked to each others by several kinds of dualities as illustrated in FIGURE 1.1

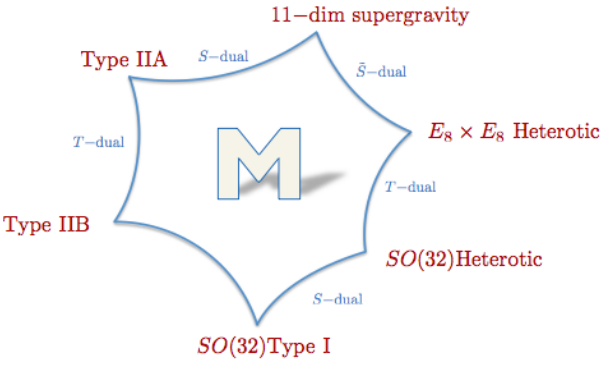

FIGURE 1.1: The duality web representing the way six string theories are linked together. This figure is taken from [2]

The holographic principle, AdS/CFT correspondence, gauge/gravity duality are the names that were given to the particularly interesting duality. In short, it is the map between semiclassical theory of gravity to the quantum field theory in one lower dimensions, as if the quantum theory is the hologram of the gravity theory. The quantum field theories that are applicable have been found in various systems, for example the quark-gluon plasma and quantum critical point.

The physics of the quantum critical point has been the main theme of the condensed matter study for some times. One of the reasons is because it seems to underly the physics of the high temperature superconductor. Aside from the technological applications, these strongly interacting systems are particularly interesting since they cannot be explained using the currently understood quantum field theory for weakly interacting systems. It seems that we need a new way to formulate the quantum field theory that gives the strongly interacting system from the start. The fact that the gauge/gravity duality gives us an accessibility to strongly correlated field theory as a starting point raises hope for understanding these classes of quantum systems.

The plan of this dissertation is the following. For chapter 2, the dictionary rules for the condensed matter are introduced together with the outline for calculate some quantities, which are more complicated to do in the standard field theory approach. The main theme of this dissertation is in chapter 3, where I will fully focus on the popular holographic models of fermions. These models includes the semi-local quantum liquid, electron star, hard wall fermi liquid and the holographic fractional fermi liquid. At the end of this review, I will discuss about recent promising works that may link together the physics of black hole, condensed matter and quantum information.

For the rest of chapter 1, I will introduce two seemingly uncorrelated physics. Firstly, I will outline the AdS/CFT correspondence from string theory point of view and explain why it can be useful. Then, a very condensed matter inclined introduction to the theory of electrons will be discussed. The aim of this section is to give motivations why some of the condensed matter systems are so hard to deal with. The second part of the condensed matter introduction is about the quantum critical point, which is the first arena of the Ads/CFT in condensed matter physics. At the end of this chapter, I will outline some features that might link these two areas together.

1.2 Decoupling argument : AdS/CFT correspondence

1.2.1 Same Physics with Two Points of Views : Baby Problem

Before starting the discussion on string theory, let's look at the problem of an electron interacting with a proton (or a chunk of quarks). If one wants to study the dynamics of this electron, they can do it in two following ways.

1. Draw Feynman diagrams including interaction vertices between quarks and the electron
2. Calculate the background electric potential created by the proton

These two methods should give the same physics with the accuracy depending on how careful we calculate the background potential. Note that we will only take into account the presence of the proton in the first picture while we only look at the background potential in the other. Moreover, when we do the calculation, we only use only one of these two pictures. Not both.

I am introducing this baby problem since it is conceptually similar to the decoupling argument I will discuss in a few lines. With this picture in your head, hopefully, I can convince you that the AdS/CFT correspondence is not some random esoteric statement from string theorists.

1.2.2 Brane and open string

Let's move from the baby QED to string theory. The role of electron in the baby problem is now played by the closed fundamental string, which looks like a very thin rubber bandThe main difference(other than the fact that closed F1 is a 1-dimensional object) is that the string F1 also interacts with graviton and other gauge field [3]. Therefore, its trajectory in spacetime forms a **world sheet** which spans in the time direction instead of a world line of a particle. In perturbative string theory, people study normal modes of this world sheet and quantise it into states with different masses and spins [4, 5]. Moreover, the spectrum of a closed string not only contains one type of particle but also several types depending on the supersymmetry of the theory[3].

The other object in this setup is called "Dp- Brane" which extend in p spatial directions and 1 time direction. We say that the p+1 dimensional space spanned by Dp-brane is the brane's **World Volume**. The D-brane is special because it allows the fundamental strings F1 to end on it. When the two end-points of the F1 are on the brane, we can say that the string has no tension(since it is not stretched) and hence massless. The string with this boundary condition is called open string. Similar to the closed string case, the open string states also represent several kinds of particles. In fact, the supercharge of the theories living on a brane is reduced from the theories in the background without a brane by half. However, I will not discuss about this in detail.

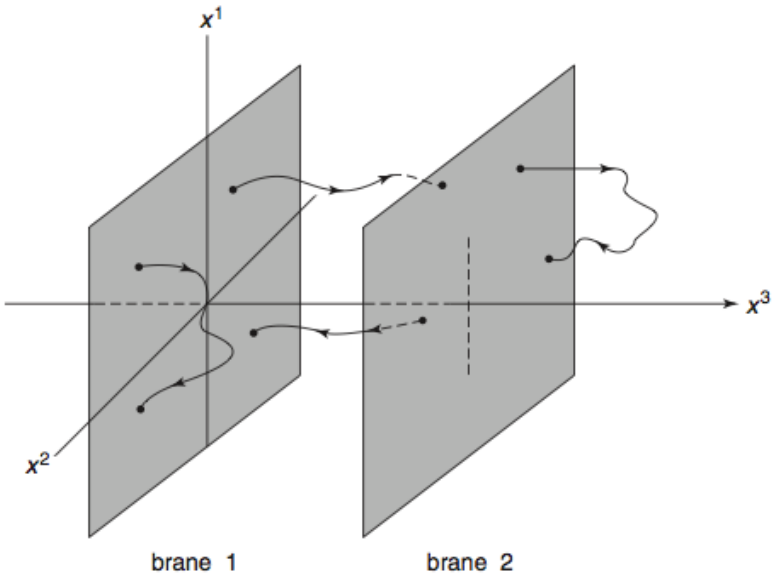

FIGURE 1.2: The illustration of two parallel D2 branes with an open string on each brane and one open string stretching between two branes. Note that the arrows represent the "chirality" of the string and different direction means different states.
This picture is taken from [6]

Now, we are going to see a bit more interesting setup from branes and string. Imagine two branes parallel to each other. There can be strings ending on each brane and strings that stretch between two branes as illustrated in FIGURE 1.2. In this figure, only the strings stretching between two branes have a tension and therefore are massive. Therefore, fields that live on each brane are massless. There are also two additional massive multiplets from two strings stretching between branes. These massless open string states include a 1-form gauge field that lives only on the brane and interacts with the end point of the massless multiplet. This interaction is similar to the U(1) gauge field coupling to the point charge particle.

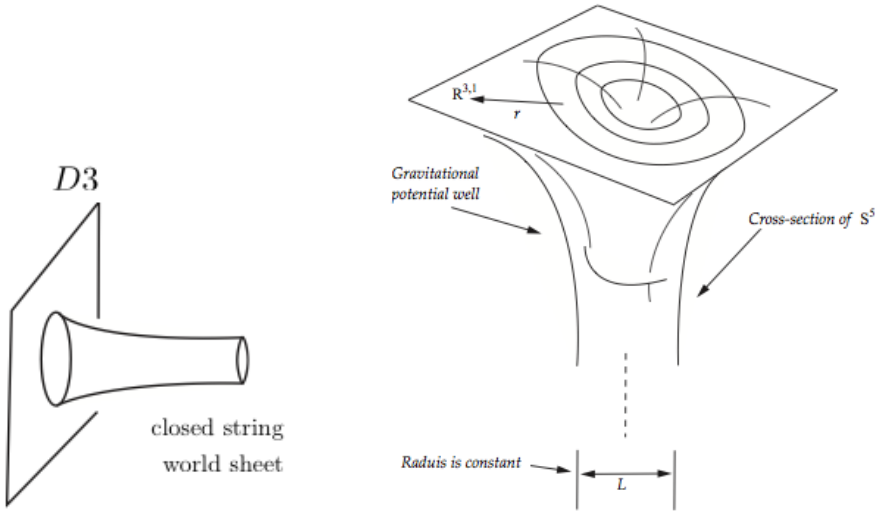

FIGURE 1.3: LEFT: The world sheet of a closed string emitted from the brane. The graviton is contained in the supermultiplet represented by the closed string
RIGHT: The flat 9+1d Minknowski spacetime deformed into $AdS_5 \times S^5$ near the brane which lives down the "throat" of this spacetime. These figures are taken from [7]

Something interesting happens when we move these two branes so that they coincide. It can be shown that the mass of the strings stretching between branes vanish (see e.g. Ref[6]). Now the massless gauge field came from 4 open strings in FIGURE 1.2. We can pack these 4 gauge fields together into U(2) gauge group. By separating the branes we break the gauge group from U(2) to U(1)×U(1), which mimicks the Higgs mechanism! This is clearly a beautiful insight from string theory. However, the feature I want to emphasise is that we can form an U(N) gauge group with large N by stacking N Dp-branes together. The stack of N Dp-branes is essential to the decoupling argument discussed in the next section.

Final comment before moving to the famous Madacena's decoupling argument is that, similar to the closed string, the Dp-brane also has mass. Thus a large number of stacked branes (which are heavy enough) can deform the spacetime it lives. This process is called a "backreaction". This can be interpret as a brane acting as source that emit gravitons as shown in FIGURE1.3.

The things I emphasise above are common knowledge from master level string theory course. Readers can find out more about these topics in e.g. [3–6]

1.2.3 Decoupling argument

Let me return to the situation similar to the baby problem discussed earlier. However, we will consider the system of a closed string and N D3-branes instead of an electron and quarks. The background spacetime of this setup becomes more exotic. Instead of working in 3+1 d Minkowski spacetime, I will consider the 9+1 d Minkowski with 32 supercharges. The string theory in this setup is called the Type IIB string theory. Similar to the baby problem, we can look at this situation from two perspectives as shown in FIGURE 1.4, namely

1. **Brane perspective**: String moves toward the stack of branes, interact, then bounces off.
2. **Spacetime perspective**: String moves in a non-trivial spacetime background(resulting from the branes' backreaction)

The world sheet of the string ending on branes has two interpretation (see FIGURE 1.4 LEFT). In the brane perspective, We can think of the ingoing closed string acting as a **source** of the open string living on the branes. The open string then propagates along the branes and vanished once the closed string bounced away. The role of a closed string as a source/sink of the open string on the brane will become an important concept when I introduce the dictionary rules next chapter.

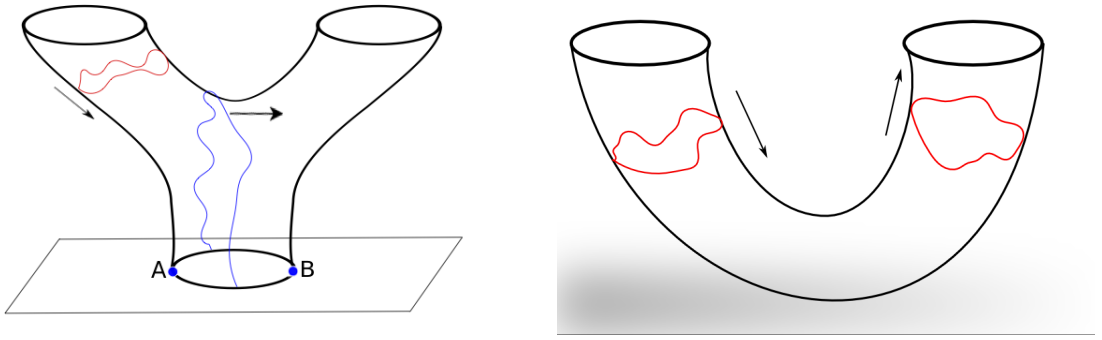

(a) String interacts with brane in brane perspective

(b) String interacts with the spacetime deformed by branes in spacetime perspective

FIGURE 1.4: LEFT: The closed string (red) moving toward the brane lying on the AB plane. The open string(blue), sourced by the incoming string propagating along the brane. RIGHT: The string propagating in the non-trivial geometry background (black shaded area).

The way to obtain the other perspective is to consider the emitted closed string that interacts with the incoming one. As mentioned earlier, the closed strings also represent the graviton and others particles due to the supersymmetry. Hence, we can say that the incoming closed string interact with the graviton emitted from the branes. This is equivalent to the situation where the incoming closed string move in non-zero gravitational potential background, which is exact the spacetime perspective defined earlier.

In order to proceed to the decoupling argument, we are interested in the massless modes which survive in a low energy limit. The action of the massless mode in brane perspective has

the form[8]

$$S = S_{bulk} + S_{brane} + S_{int} \tag{1.1}$$

S_{brane} is the action of the field living on the brane. S_{bulk} is the action of the closed string in the $\mathbb{R}^{9+1}$ background. If we only consider the string's low energy excitation, these actions will become the $\mathcal{N} = 4$ super Yang-Mills action and the Type IIB supergravity action respectively. The theory with higher energy will require higher order derivative terms as a correction to the $\mathcal{N} = 4$ and Type IIB action. Note that the $\mathcal{N} = 4$ super Yang-Mills theory is special in the sense that it is the field theory that preserves conformal symmetry (thus called **conformal field theory or CFT**). More details and definitions of CFT can be found in[8, 9] or [10]

On the other hand, with the spacetime perspective, the closed string at low energy is also described by the supergravity action. The difference from the branes perspective is that, here, we no longer 'see' the branes but have the supergravity in the curved background, which formed by the stack of D3-branes. This spacetime is depicted in FIGURE1.3 and described by the metric[7, 8, 11]

$$ds^2 = \frac{1}{\sqrt{H(u)}} \underbrace{\left(-dt^2 + dx^i dx^i\right)}_{\mathbb{R}^{3+1}} + \sqrt{H(u)} \underbrace{\left(du^2 + u^2 d\Omega_5^2\right)}_{\mathbb{R}^6} \tag{1.2}$$

with

$$H(u) = 1 + \frac{L^4}{u^4}; \qquad L^4 = d_p \, l_s^4 \, (g_s N)$$

where d_p is some numerical factor and g_s is the string coupling (which is inversely proportional to the amplitude for the closed string from D-brane) [7, 8]. We can see that when $u \to \infty$, the metric become Minkowski space $\mathbb{R}^{9+1}$. While in $r \ll L$, the metric will have the form

$$ds^2 = \frac{u^2}{L^2}(-dt^2 + dx^i dx^i) + \frac{L^2}{u^2} du^2 + L^2 d\Omega_5^2 \tag{1.3}$$

The last term on the right-hand side describe the 5-dimensional sphere S^5 with the radius L as labelled in FIGURE1.3. The first two term is the spacetime called 5-dimensional Anti de-Sitter space (AdS_5). This is exactly where the AdS part in the AdS/CFT came from. The picture of this spacetime is the part down the "throat" in FIGURE1.3 -RIGHT.

We are now very close to the decoupling argument story. Let's compare what we have in both brane and spacetime pictures.

Brane Perspective	Spacetime Perspective
Open string lives on the branes described by S_{brane} part	Closed string propagating in 'throat' at $u \ll L$
+	+
Closed string lives in the flat background described by S_{bulk} part	Closed string lives in the flat background at $u \gg L$

I have to emphasise that both brane/spacetime perspective describe the same physical system. The situation here is very similar to what we discussed the baby problem, despite a lot more enigmatic buzzwords. Here we can see that there are something peculiar. Both pictures

have two sectors. One of the sectors in both picture is closed string in the flat background. These two sectors are not separated, of course. Their interaction indicated by the presences of S_{int} in the brane perspective action and, in the spacetime perspective, the fact that the closed string can propagate back and forth between $u \gg L$ and $u \ll L$ regions.

But it is known that AdS spacetime is the solution of the Einstein field equation with negative gravitational constant [7, 12]. So there is a possibility that the string at $u \gg L$ propagating toward $u \ll L$ is unable to reaches the region $u \ll L$ due to the pressure created by the gravitational constant term. This statement can be made more explicit in [8] and the references therein, which consider the low energy absorption crossection. The form of this crosssection is $\sim E^3 L^8$. The small absorption at low energy mode (with small E) indicate that the low energy string in asymptotically flat background at $u \gg L$ hardly reaches the $u \ll L$. Furthermore, we notice that the factor u^2/L^2 in the metric (1.3) where $u/L \to 0$ cause an infinite redshift as if $u = 0$ is an event horizon. This type of horizon is called **the Cauchy horizon** or **the Poincaré horizon**. Hence, the string excitations near the Poincaré horizon, which can be high energy excitations, suffer from the redshifted and become low energy excitations to the observer at large u. For the observers in the asymptotically flat region, the local high energy excitations near the Poincaré horizon become infinitely redshifted and are unable to interact with the closed strings in the region $u/L \to \infty$.

What does this means! It means that we may tune parameters in the theory such that the two string sectors not "talk" to each other. Since we can ignore the interaction between the two sectors, we say that the string in $AdS_5 \times S^5$ ($u \ll L$) and the string in $\mathbb{R}^{9+1}$ ($u \gg L$) are **decoupled**. It is natural to suspect that, in the brane perspective, the open string and the closed string sectors may decoupled as well. And indeed, it is. [7, 8, 11]

Back in 1997, Maldacena proposed this insightful conjecture that **we can then ignore the closed string part that living in flat spacetime in both perspectives** [13]. Thus what we have left is the physical physical situation that can be described by the two different physics. The field theory describing the open string living on the brane world volume corresponds to the supergravity describing closed string propagating in $AdS_5 \times S^5$! In short, we say that **these two theories are dual of each others**. It is definitely not so obvious but both pictures indeed represent the same physics!

1.2.4 Do they really decoupled ?

We just finished a section of handwaving introduction of the AdS/CFT correspondence. Now I will examine what limits we are working on and explain what do they mean.This is a standard discussion which I include for completeness of the dissertation. Similar materials can be found from standard AdS/CFT review articles e.g. [7, 8, 11] or, for brave, [9].

In the spacetime perspective, we have the Type IIB supergravity action with metric g_{MN}, the 2-form field strength $F_{\mu\nu}$, which lives on the branes' world volume, and the dilaton ϕ, which

$\phi \to 0$ at large u. The action has the following form.

$$S = \frac{1}{2\kappa^2}\underbrace{\int d^{9+1}x\sqrt{-g}\left[\mathcal{R} - \frac{1}{2}(\partial\phi)^2\right]}_{\text{whole spacetime}} - \frac{1}{4}\underbrace{\int d^{3+1}x\left[e^{-\phi}\mathrm{Tr}F^2\right]}_{\text{D3-brane world volume}} + \dots \tag{1.4}$$

At low energy limit, we don't want the string to oscillate too much. Therefore, the string tension, which is inversely proportional to the string length scale l_s (or sometimes written as $\sqrt{\alpha'}$) has to be very large compare to the other energy scales in the theory. However, there is only one other length scale namely the radius L of the sphere S^5. Therefore, we have

$$L \gg l_s \quad ; \quad L^4 \propto O(g_s N) \tag{1.5}$$

The stack of branes must be heavy to ensure that a stack of branes is heavy enough to backreact the spacetime into $AdS_5 \times S^5$. Let us consider the equation of motion

$$R_{MN} \sim \kappa^2 \tilde{F}_{MABCD}\tilde{F}_N^{ABCD} \tag{1.6}$$

The constant $\kappa^2 = g_s^2\, l_s^8$ plays the role of Newton's gravitational constant in 9+1 dimension[7, 8]. We can read off the number of branes by looking at the flux of the field strength 5-form $\tilde{F}_{ABCDE}$ that sources the branes. This is in fact similar to Guass law, which the electric field $E \propto$ the charge Q. The field strength is therefore proportional to the number of branes $\tilde{F} \propto N$. We also know that the The Ricci tensor $R_{MN} \propto L^8$ by either dimensional analysis, or plugging in the solution (1.2) into the Einstein equation (1.6). Putting all these together the equation (1.6) becomes

$$\frac{L^4}{l_s^4} = g_s N \equiv \lambda \gg 1 \tag{1.7}$$

The parameter λ is usually referred to as the 't Hooft coupling. Now, let's see what will happen if we take these limits.

1. The higher derivative terms in both S_{bulk} and S_{brane} in both perspectives must be dimensionless. Thus they must proportional to the string scale l_s and suppressed in the low energy limit [11]. Therefore all the fields in the bulk are massless and the theory on brane/bulk becomes $\mathcal{N} = 4$ super Yang-Mills/ Type IIB supergravity.

2. For a large but finite λ, we can see that $\kappa^2 \propto 1/N^2$. This means that the gravity in the bulk can be treated semiclassically for a large value of N (sometimes called **Large N limit**). In this limit, the complicated quantum gravity effect can be ignored.[7, 8]

3. In the brane picture, we can expand the metric around the flat background (since the spacetime is flat in this picture) as $g \sim \eta + \kappa h$. The interaction term S_{int} becomes [11]

$$S_{int} \sim \kappa \int d^4x \mathrm{Tr}\left(F_{\mu\nu}^2 - \frac{\delta_{\mu\nu}}{4}F^2\right) \to 0$$

in the large N limit, where F is the 2-form field strength. The string on the branes and the string in the flat background have decoupled as advertised.

Let me end this section by showing you a glimpse of how this duality might be useful. The physics of the D3-brane tell us that the string coupling is related to the Yang-Mills coupling in $\mathcal{N} = 4$ super Yang-Mills as $g_s \sim g_{YM}^2$. We know that in the limit of large N and g_{YM}, the gravitate in the dual theory is semiclassical. **This suggest that we might be able to study the strongly interacting quantum theory with a weakly semiclassical theory of gravity!** Due to the correspondence between brane perspective and spacetime perspective, I will refer to them as field theory side and gravity side respectively.

What kind of field theory we can study with this duality other than $\mathcal{N} = 4$ super Yang-Mills with SU(N) gauge group? The early application in 2001 found a surprisingly match between experimental results of quark-gluon plasma and the AdS/CFT prediction [2, 14]. The result from the AdS/CFT analysis and from the experimental are strikingly similar despite the fact that the quark-gluon plasma is described by QCD, which only has SU(3) gauge group and no supersymmetry. The applications in condensed matter system started to appear in 2007[15]. But what kind of condensed matter system is applicable? and why should we interested in such system? I will illustrate these points in the following section.

1.3 The Landau Fermi liquid theory and Quantum Phases Transitions

1.3.1 Robustness of the Fermi liquid theory

The Fermi liquid theory is essentially the theory of electrons in metal, which is mainly a composition between electrons and a lattice. We have learned from the undergraduates physics that N electrons in d dimensions fill the states with momentum lower than $k_F \sim N^{1/d}$ and only the portion of electrons near k_F (called the Fermi surface) contributes to the thermodynamics. Surprisingly, a lot of features of the metal are obtained by the model of non-interacting electrons in a box, called the Sommerfeld - Bloch model [16, 17]. It is very peculiar that this model works so well since the electrons are strongly interacted, via Coulomb interaction. The resolution to this problem is that the Coulomb interaction is screened when we have a dense electrons system [16, 18]. Let's consider the system with an electron density $n = N/L^d$. The Coulomb potential is $\sim n^{1/d}$ due to the fact that the electron spacing is $1/n^{1/d}$. The kinetic energy of the quantum oscillation for an electron on the Fermi surface is $\sim \hbar^2 k_F^2/2m \sim n^{2/d}$. The ratio of these two energies is

$$\frac{\text{Coulomb energy}}{\text{kinetic energy}} \sim \frac{1}{n^{1/d}}$$

which goes to zero as $n \to \infty$. Further explicit field theory calculation showing that the electrostatic potential takes the form $e^{-k_F r}/r$ can be found in [18]. This indicates that the electrostatic interaction is subleading and can be treated as a perturbation to the free electrons.

The theory of the Landau-Fermi liquid is the following. Free electron parameters (e.g. mass) are corrected by the quantum correction from the interaction terms. The excitation on the Fermi surface are no longer electrons (and holes) but a new entity called quasi-particles

given that states of quasi-particle have a one-to-one correspondence with the states of the non-interacting Fermi gas[16]. To guarantee that behaviour of the quasi-particle is exactly the same as in the non-interacting ones, we need all interactions to be irrelevant. We start with the free nonrelativistic Dirac Lagrangian and then add the interaction terms order by order. If there is no marginal or relevant term according to Wilsonian renormalisation scheme, our theory works. In the absence of a lattice, it turns out that all the interaction terms are irrelevant. This can be seen by writing the action with all possible interactions and scale the momentum by $s > 1$[1]. We can see that the action takes the form [2, 19]

$$\begin{aligned}\mathcal{S}_{\text{Fermi Liquid}} &= \int dt \int \frac{d^d k}{(2\pi)^d} \left[\psi_\sigma^\dagger \left(i\partial_t - v_F(k-k_F) + \frac{\alpha}{s}\omega^2 + \frac{\beta}{s}(k-k_F)^2 + \dots \right) \psi_\sigma \right. \\ &\quad \left. + \sum \frac{1}{s^{jd}} (\psi^\dagger \psi)^{j+1} \right] \end{aligned} \tag{1.8}$$

Here σ is the spinor index and s is the scale factor defined in[19]. We can see that the Lagrangian is reduced to the Dirac Langrangian if we follow the RG flows to $s \to \infty$. Thus all added terms are irrelevant. At finite s, the electron's parameters are renormalised. In this case the field ψ is no longer describing the free electron but the Landau quasi-particle.

According to [20], the Fermi liquid can be regarded as the fixed point where all the perturbations away this theory flow back to. This makes the Fermi liquid theory very robust since none of the perturbation are relevant[2] It seems that, with this starting point, we cannot build any metallic states other than the Fermi liquid. This would be very boring since it means we have found the theory of all metal. Fortunately, it is not true and a counter example is present in the next section

1.3.2 Signature of the (non-)Fermi Liquids

The signature of the Fermi liquid theory (1.8) has a robust effect on the retarded Green function and the metal's transport properties. From (1.8), the form of the Green function is restricted to be

$$G_R^{-1}(\omega, \mathbf{k} \to \mathbf{k_F}) = \omega - v_F|(\mathbf{k} - \mathbf{k}_F)| + \Sigma(\omega, \mathbf{k}) \tag{1.9}$$

with $\Sigma \sim \omega^2/M$ comes from the leading term in the expansion (1.8). The term Σ is interpreted as the decay rate of the quasi particle. The ω^2 dependence implies that the decay rate is very low for the low energy excitation. Thus the quasi particle is long lived. This is a reasonable prediction, otherwise there would be no charge carriers in the metal.

Knowing the form of the Green function, one can shows that the specific heat of the metal is linear in temperature and the low temperature resistivity increases quadratically[2, 16, 21]

$$C_V \sim T\,; \qquad \rho(T) \sim \rho_0 + AT^2 \tag{1.10}$$

[1] According to[19], $t \to t/s$, $k \to sk$ and $\psi \to s^{-\frac{1}{2}}\psi$ for 3+1 spacetime. Note that the momentum k parallel to the Fermi surface is not scaled.

[2] Note that, with the lattice, the term $(\psi^\dagger\psi)^2$become marginally relevant and we get the standard low-temperature superconductor.

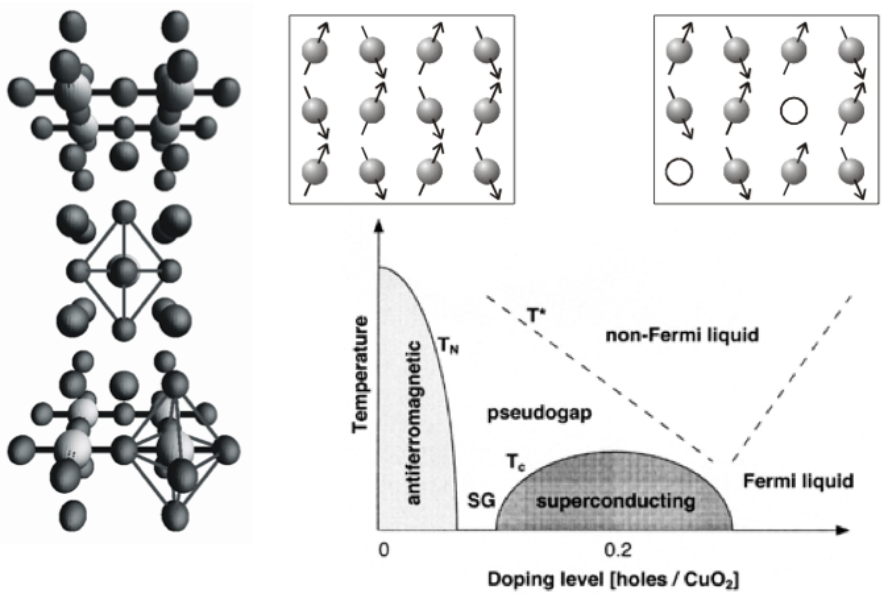

FIGURE 1.5: **LEFT** The atomic structure of the Lanthanum cuprate. **RIGHT** (**Top Left**) Electrons struck on the plane and their spins exhibit antiferromagnetic properties. They are able to move around once we increase the doping (**Top Right**). (**Bottom**) The phase diagram of the curprate. Even at zero temperature, the electrons can be driven into the states other then metal i.e. antiferromagnet, spin glass (SG) and the superconductor. The strange metal phase, called pseudo gap and non-Fermi liquid, are found at non-zero temperature. This picture is adapted from [22] but the phase diagram is replaced by the updated one from [24]

If the Landau-Fermi liquid theory is the theory of all metals, then all of them should obey (1.10). This is very easy to verify that it is not true.

The famous counter example is the copper oxide compound called "**cuprate**" shown in FIGURE 1.5. In this material, free electrons are confined in 2-spatial dimensional layers. The other atoms act as some sort of scaffolding keeping these layers apart. The pristine state of the cuprate is the **Mott insulator** where the electrons are stuck in the plane and unable to move. We can obtain the different phases by removing the electrons on the plane - a process called **doping** [22]. As a result, many phases, including the Fermi liquid, are obtained by doping and increasing temperature as shown in FIGURE1.5. This compound receives a lot of attention due to the existence of the **"superconducting dome"** that extends to a much higher temperature (about 150 K) than the well-understood superconductor, which only exist below about 30 K [23]. The existence of the high temperature superconductor leads to the hope that we might be able to obtain the superconductor at the room temperature! However, I will focus on a the theoretical issue regarding how the Fermi liquid can be driven into so many different phases since all perturbations are irrelevant.

The hint is actually in the RG analysis [20]. It is true that all perturbation theories flow back to the Fermi liquid fixed point. But what about non-perturbative theories with strong interactions? Since they don't have to flow toward the Fermi liquid fixed point, they may correspond to the exotic phases in the phase diagram of the cuprate. We might hope that we will be able to extract some physics from non-perturbative methods like Monte-Carlo simulation in lattice field theory.

However, simulating fermions is not as simple as bosons, which is already difficult. The problem is referred to as "**the sign problem**". This can be illustrated by looking at how we calculate the partition function.[25, 26]

$$\mathcal{Z} = \mathrm{Tr}\, e^{-\beta H} \sim \sum_{\text{all possible path}} e^{-S[\text{path}]} \tag{1.11}$$

This can be generalised to N-body problem by changing $e^{-S} \to \rho(\mathbf{R};\mathbf{R})$ where $\mathbf{R} = (\mathbf{r_1}, \ldots, \mathbf{r_N})$ denotes the positions of N particles and $\rho(\mathbf{R}_{\text{initial}};\mathbf{R}_{\text{final}})$ denotes the density matrix. For bosons, it does not matter how many particles you have since we don't have to simulate all permutations $\mathbf{R} \to \mathcal{P}\mathbf{R}$. Fermions have a completely different story. The odd permutations will result of negative density matrix, due to the quantum statistic. Such permutations are not allowed since they are result in a negative probability that particles will follow these paths. Computers need to simulate each path and each permutation one by one to figure out which one has a negative probability. It turns out that the number of computational processes grows as non-deterministic polynomial function of N [25]. This kind of simulations for a realistic number of electron cannot be done by any classical computers since, even for only a few hundreds electrons. This is because the numbers of computational processes of such simulations can be much larger than the estimated number of atoms in the universe! [27]

So in order to obtain phases of strongly interacting fermions from our current understanding, we need to somehow bypass the brick wall of the sign problem. This is a very challenging theoretical problem since none of our existing tools works, both perturbation and computer simulation.

My focus in this dissertation is the non-Fermi liquid region above the Fermi liquids. Intuitively, by heating up a piece of metal, we should simply get a hotter one and expect no phase transition. However the transport properties of this region are significantly different from those predicted by the Landau-Fermi liquid theory. Phenomenological studies indicate that transport properties of this strange metal can be obtained if the decay rate Σ took the form [21, 28, 29]

$$\Sigma(\omega, \mathbf{k} = \mathbf{k}_F) = \omega\,(c \log \omega + d) \tag{1.12}$$

where c is real and d is complex. How could this form of decay rate appear ? People haven't figured it out yet. The other clue is that the phase boundary of non-Fermi liquid looks like some kind of 'chinese fan' attached to the superconducting dome. This might have something to do with the phase transition driven by quantum fluctuation at zero temperature.[30]

1.3.3 Quantum phases transition : a very short introduction

Recall that, in the phase transitions we learned in the standard quantum field theory course, we assumed that the mass term $m^2|\phi|^2$ in the complex scalar field theory is proportional to $a(T - T_c)|\phi|^2$. For $T < T_c$, the mass term becomes negative and signals an instability. The scalar field (e.g. Higgs field) therefore condensates i.e. $\langle\phi\rangle \neq 0$. This non-zero expectation value spontaneously break the U(1) symmetry, $\phi \to e^{i\theta}\phi$, where $\theta \in \mathbb{R}$. Thus the symmetry group of

the condensate phase $\langle\phi\rangle \neq 0$ has to be a subgroup of the unbroken symmetry phase $\langle\phi\rangle = 0$. The scalar expectation value is usually called **order parameter** since it is non-zero in more ordered phases (with less symmetry) and vanish in disorder phase (with more symmetry). This treatment of phase transitions is normally referred to as Ginzburg-Landau formalism.

We will look at a model to which the above formalism cannot be applied. It is a simple model of a repulsive bosons on the periodic potential well (referred to as the Hubbard model) with the Hamiltonian [31–33]

$$\mathcal{H} = -t\sum_{\langle ij\rangle}(\hat{b}_i^\dagger\hat{b}_j + \hat{b}_j^\dagger\hat{b}_i) + (U/2)\sum_i \hat{n}_i(\hat{n}_i - 1) \tag{1.13}$$

with $\hat{b}_i$ is the annihilation operator, $\hat{n}_i = \hat{b}_i^\dagger\hat{b}_i$ denotes the number operator of the bosons on the site i, t measures the tunnelling amplitude for bosons from site i to j and U corresponds to the repulsive potential between two bosons on the same site. By tuning the ratio $g = U/t$ we see that we can obtain two different ground states, even at zero temperature. For $g \ll 1$, the tunnelling between sites dominates and the bosons becomes superfluid as if there was no potential barrier. For $g \gg 1$, the tunnelling is suppressed and there is only a single boson stuck at each site (so this state is a Mott insulator). There will is a critical value of $g = g_c$ where the phase transition between the Mott insulator and the superfluid occurs. Since this transition has nothing to do with the thermal fluctuation, unlike the Ginzburg-Landau formalism, it is called a"**quantum phase transition**". The phase diagram of this model is shown in FIGURE1.6.

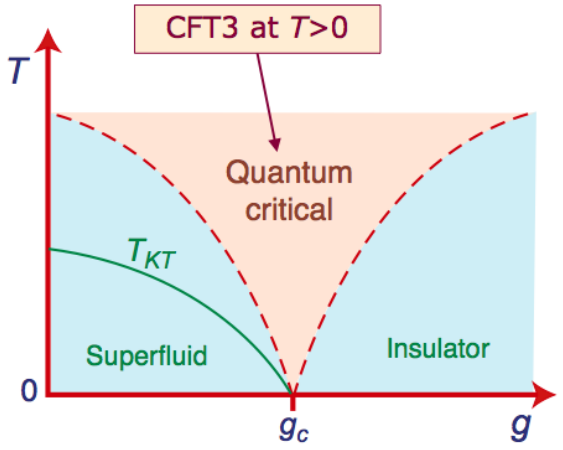

FIGURE 1.6: The phase diagram of the Bose-Hubbard model. The critical value of $g = g_c$ indicates the phase transition at zero temperature. This picture is taken from [17]

This phase transition has a lot of interesting features. First of all, unlike the thermal phase transition, the symmetry of one phase is not a subgroup of the other phase. The superfluid completely breaks rotational symmetry but not translational symmetry while the insulator breaks translational symmetry but does not completely break rotational symmetry. Also, the characteristic length scale of this system diverges as $g \to g_c$. Hence the quantum critical point $g = g_c$ is scale invariant. One can show that this critical point also has a conformal symmetry [33], similar to $\mathcal{N} = 4$ super Yang-Mills, except no supersymmetry.

For the purpose of my dissertation, there are two additional key features I would like to emphasise. Namely :

1. We notice that the quantum critical region looks remarkably similar to the non-Fermi liquid region in FIGURE 1.5. Further studies[17, 31] show that the relaxation time of quantum critical fluid takes the form

$$\tau \quad \propto \quad \hbar/k_B T \tag{1.14}$$

   The $\hbar$ dependence indicates that the quantum behaviour survives under a low thermal fluctuation. Moreover, the peculiar ratio $\hbar/k_B T$ also appears in the semiclassical theory of gravitational wave near black hole horizon[34] and the application of AdS/CFT in the quark-gluon plasma[14]. Could it be that the theory of gravity also knows something about quantum criticality?

2. Both quantum critical region and non-Fermi liquid 'fan' seems to emerge from the low temperature phase. In the Hubbard model, we can identify that the critical 'fan' emerges from the quantum critical point $g = g_c$. Perhaps the origin of the quantum critical phase is from the quantum behaviour that we are not quite understand at the quantum critical point. This point will be discussed in a bit more details in the next section.

1.3.4 What could happen at quantum critical point?

At the time we studied quantum field theory, quantum behaviour is treated as a random fluctuation, in the same way that the thermal fluctuation is treated in statistical mechanics. The term quantum entanglement is rarely mentioned. However, quantum entanglement seems to play a crucial role in the story of quantum phase transition [17]. Let us consider the model of quantum phase transition where the entanglement is more apparent. The following Hamiltonian describes spins sitting on a 2d triangular lattice where their nearest neighbours prefer to point in opposite directions [17, 32].

$$\mathcal{H} \quad = \quad \sum_{\langle ij \rangle} sJ S_i^z S_j^z + J(S_i^x S_j^x + S_i^y S_j^y) \tag{1.15}$$

Similar to the Hubbard model, we obtain the quantum phase transition by tuning the dimensionless parameter s. For $s \ll 1$, the first term can be ignored and the interaction of spins in xy-components dominates. The spins form the antiferromagnetic long-ranged ordered state as shown in FIGURE 1.7 (LEFT). With $s \gg 1$, the interaction of the z-component dominates. The spins in the nearest neighbour site form a singlet pair $(|\uparrow\rangle \pm |\downarrow\rangle)/\sqrt{2}$. This is a disordered state since there is only short ranged correlation between two spins on the nearest neighbour sites. Note that, once two spins form a singlet pair, they are entangled.

In order to understand what happens to the entangled pairs when we smoothly tune $s \to s_c$ so that the system is scale invariant? I will discuss the quantity that can provide us some information about quantum entanglement, namely entanglement entropy S_E.

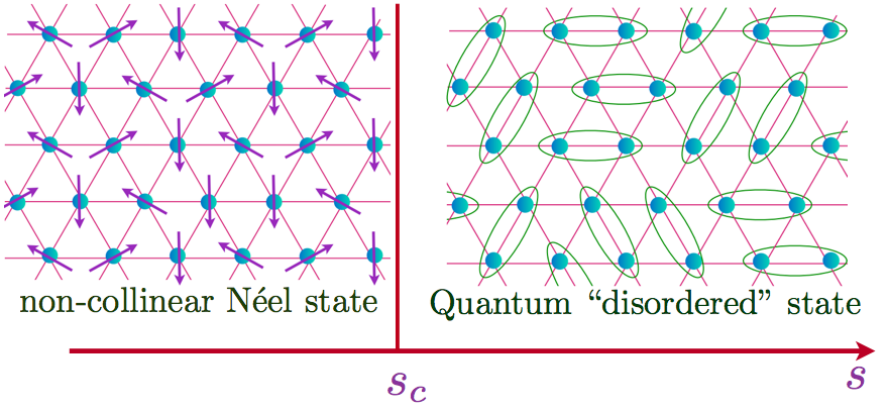

FIGURE 1.7: The phase diagram of antiferromagnet model at zero temperature. The ordered Neel state occurs when $s < s_c$ while the quantum disorder state is located at $s > s_c$. A dimer on the quantum disordered state indicate the singlet pair $(|\uparrow\rangle \pm |\downarrow\rangle)/\sqrt{2}$ between two spins it encircled.This figure is taken from the talk by Subir Sachdev at Imperial College in 2012 [35]

Given the wave function of the whole ground state, $|\Psi\rangle$, we can calculate S_E from the following procedures [17]. First, divide the system into two subsystems, A and B. Then trace over the spin in region B to obtain the reduced density matrix $\rho_A = \mathrm{Tr}_B\left(|\Psi\rangle\langle\Psi|\right)$. Hence, we obtain the entanglement entropy through the formula $S_E = -\mathrm{Tr}(\rho_A \ln \rho_A)$. It is straightforward to show that $S_E = 0$ when there is no entanglement between regions A and B, i.e. when $|\Psi\rangle = |\Psi_A\rangle \otimes |\Psi_B\rangle$. This makes S_E a good measurement for quantum entanglement although the actual calculation is really difficult and there are very few constrained systems where analytic calculation can be done [36, 37].

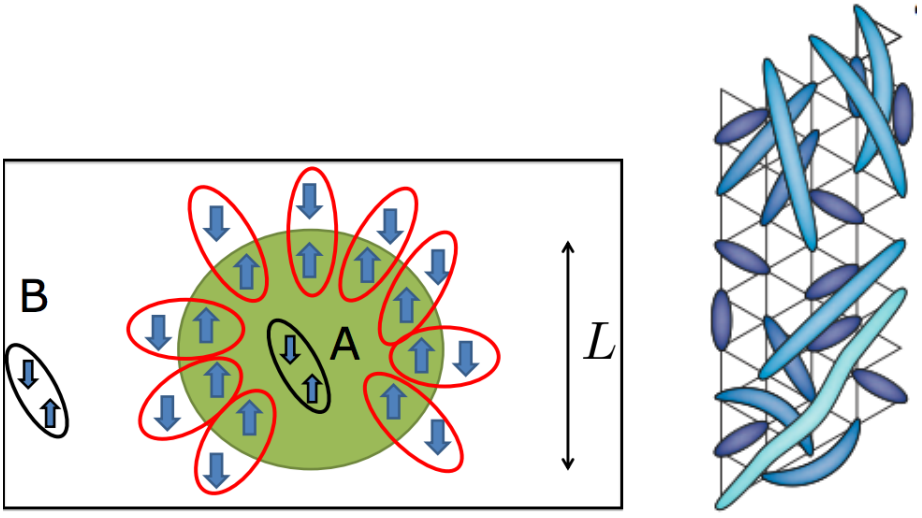

FIGURE 1.8: **LEFT**: Subsystems A and B in the quantum disordered state. The red dimers represent the entangled pairs between spins in the region A and B. **RIGHT**: The illustration of long-ranged entangled pairs at the quantum critical point.These figures are taken from [38] and [32] respectively

The form of S_E for our spin model is expected to obey the boundary law that is

$$S_E = \alpha L - \gamma \tag{1.16}$$

where L is the diameter of the boundary between region A and B, α is some constant and γ is a universal constant. In the disordered state $S_E = \alpha L$ is is proportional to the perimeter of the region A. Thus, we can say this S_E counts the number of entangled pairs between A and B (see FIGURE 1.8 - LEFT). However, at $g = g_c$, the constant γ turns out to be non-zero. This indicates that there are long-ranged entangled pairs between spins in the deep interior of A and B. The illustration of this situation is shown on the RHS of FIGURE 1.8. More details about obtaining (1.16) can be found in [17, 36] and the reference therein.

Before ending this preliminary chapter, I want to emphasise that doing a strongly correlated electron system is hard. The quantum criticality, which seems to underly the physics of the cuprate, is complicated and has a lot to do with the quantum entanglement. It will be very exciting if there is a gravity dual, not only for the $\mathcal{N} = 4$ SYM, but also the quantum critical point. The calculations in the dual theory, which is a semiclassical theory of gravity, are much less complicated than in the strongly interacting and highly entangled many-body systems.

This excitement actually happened about six years ago. The Harvard group leaded by Subir Sachdev[3] considered the dyonic blackhole as a dual theory of the quantum critical fluid in the perpendicular magnetic field background. The system exhibits the electric current when the temperature gradient is applied. This phenomena is called the Nernst effect. Surprisingly, the theories from both sides yielded almost the same transport properties! [39] Since then, features of the condensed matter's exotic phases, not just the quantum critical fluid, have been reproduced by dual gravity theories. These works have become substantial evidences that AdS/CFT conjecture is also applicable in many field theories. It is really a mind-blowing to see that the complicated structures of quantum systems are encoded in the geometry of the spacetime and to see that there are so many things we don't know.

[3]together with Markus Műller, on condensed matter side, Pavel Kovtun and Sean Hartnoll, on string theory side

Chapter 2

Holographic dictionary

In this chapter, I will introduce the essential ingredient of the gauge/gravity duality, the dictionary rules. There are two approaches to construct these rules namely top-down approach and bottom-up approach. The top-down approach starts from the gravity embedded string theory whose the dual field theory is known. The great advantage of this approach is that we will know for sure which field theory is dual to which theory of gravity. However, there are two main downsides. First of all, the string theories, where the desired gravity theories are embedded, are much more complicated than those obtained from the bottom-up constructions. Secondly, there exist too many ground states and setups in string theory. Different ground state of different setup corresponds to the different theory of gravity. These ground states are often referred to as **the string landscape** [2, 40]. Since the string landscape is too big, it is very difficult to pin point the string theory set up that gives the vacuum which corresponds to the field theory we are interested in. Nevertheless, there are a lot of top-down models that are able to capture the physics of condensed matter system and quark-gluon plasma. The interested reader can find out more about some famous top-down model such as superconductor state in [41–43], fermionic response in [44, 45], quantum hall effect in [46] and spatial modulated phase in [47, 48]. The review about the top-down constructions using Dp/Dq branes intersection can be found in[49].

In this review, I focus on the bottom-up approach where we start from AdS spacetime without any other fields. Then try to modify the theory of gravity by adding a few contents until we see the properties that agree with or resemble the results from experiments. This might sounds a bit vague but one can argue that bottom-up gravity theories are somewhere in the string landscape as ground states of the some string theory setups. The bottom-up theories of gravity are relatively simple compare to those obtained from top-down and a number of interesting condensed matter systems can be realised by adding a few field contents to the asymptotic AdS space.

The plan of this chapter is the following. Firstly in section 2.1, I show the match the symmetry of $AdS_5 \times S^5$ space and superconformal field theory. Then, in section 2.2, the mapping between fields in the gravity side and gauge invariant operators in the field theory side are discusses. In section 2.3, I will show how to calculate the correlation functions for the bottom-up

model with only the graviton and the scalar field . The correlation functions discussed here are essential to the bottom-up approach since we can compare them to the experimental results. Then, I outline how to turn on the temperature, density, electric field and magnetic field in section 2.4 and 2.5. Finally, I will discuss the notion of confining/deconfined phase transition and the entanglement entropy in the dual gravity theory.

2.1 Matching Symmetries

For the two theories to be equivalent, there must be a map between the symmetry group from one theory to the other. Here, we start with the symmetry of the $\mathcal{N} = 4$ super Yang-Mills, which is a conformal field theory. By definition, the conformal group consists of translation, Lorentz tranformation, scaling or dilatation and special conformal transformation [7–10]. The generators correspond to these transformations are

$$\begin{aligned} \text{Translation}: P_\mu &= -i\partial_\mu && (2.1)\\ \text{Lorentz}: M_{\mu\nu} &= i(x_\mu\partial_\nu - x_\nu\partial_\mu) && (2.2)\\ \text{Dilatation}: D &= ix^\mu\partial_\mu && (2.3)\\ \text{Special Conformal}: K_\mu &= -i(x^2\partial_\mu - 2x_\mu x^\nu\partial_\nu) && (2.4) \end{aligned}$$

We can compute the commutation relations between these generators and see that for conformal algebra in $\mathbb{R}^{p+q}$ is equivalent to SO(q+1,p+1) algebra [7]. Thus, for the theory lives on D3 branes, we have SO(2,4) as a conformal group. Also, we note that the vacuum of supersymmetric field theory on a D3 brane is degenerated and described by six scalar fields denoted by X^i where $i = 1, \ldots, 6$. These scalar field can transform into each other under the group SO(6). The symmetry between X^i's is normally called R-symmetry.

The AdS_5 spacetime can be considered from two points of view. The **global** AdS_5 is defined as a hyperboloid embedded in $\mathbb{R}^{4+2}$ namely

$$Y_{-1}^2 + Y_0^2 - \sum_{a=1}^{4} Y_a^2 = 1 \qquad (2.5)$$

We can clearly see that this surface is invariant under SO(2,4) transformations [7–9]. Note that the AdS solution in (1.3) or the **Poincaré patch** can be obtained from the global AdS by taking a map

$$Y_{-1} + Y_4 = L/r > 0 \quad ; \quad Y^\mu = (L/r)x^\mu \qquad (2.6)$$

with $r \equiv L^2/u$ in the original metric (1.3) [7]. On the other hand, the sphere S^5, in $AdS_5 \times S^5$, is invariant under the SO(6) group. In a more formal language, we say that SO(2,4) and SO(6) are the isometries of the AdS_5 and S^5 respectively. We can now see that both sides have exactly the same symmetry. Therefore, the first dictionary rule is established as following

SO(2,4) as CFT global symmetry	$\Leftrightarrow$	SO(2,4) as Isometry of AdS_5
SO(6) as global symmetry between X^i's	$\Leftrightarrow$	SO(6) as Isometry of S^5

The special conformal transformation will be neglected from this point onward since it can be obtained from the combination between inversion and translation. To identify the generators of Poincaré group and dilatation, we should look at the metric of the Poincaré patch i.e.

$$ds^2 = \frac{L^2}{r^2}\left(dr^2 + dx^\mu dx_\mu\right) \tag{2.7}$$

It is not difficult to see that the Poincaré patch looks like a tower of copies of Minkowski spaces with a characteristic length of each copy scaled by (L/r)

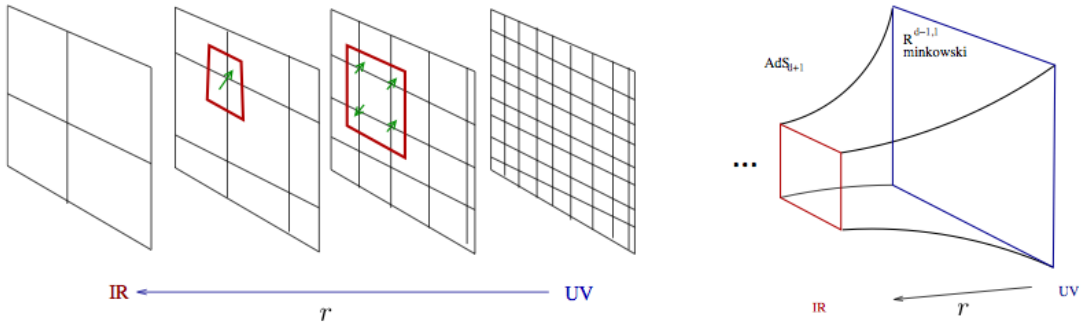

FIGURE 2.1: Comparison between tower of copies of Minkowski space at different values of r and the AdS_5 spacetime. This figure is adapt from [50]

These copies of Minkowski space are invariant under the Poincaré group transformations but not the dilatation. Thus, the isometry of a hypersurface $r = \text{const}$ corresponds to the Poincaré symmetry on the CFT side. To obtain the isometry corresponds to the dilatation, we use the fact that the AdS_5 spacetime is invariant under the dilatation. This require r to transform as

$$r \to \lambda r \quad \text{for} \quad x^\mu \to \lambda x^\mu$$

These maps between generators gives the second dictionary rule

Poincaé group in CFT	$\Leftrightarrow$	Isometry of $z = \text{const}$ hyper surface
Dilatation $x^\mu \to \lambda x^\mu$ in CFT	$\Leftrightarrow$	Traslantion from $r \to \lambda r$

If we regulate each Minkowski slice into a lattice, we will see that the Minkowski slices at small r have a small lattice size (see FIGURE 2.1). The field theory that lives on these slices are able to probe the small structure and is said to have high energy. On the other hand, the field on the slices at large r can only probe the large structure and so have lower energy. Therefore, the AdS space has been thought of as a geometric realisation of the renormalisation group(RG) flow between UV and IR region [51, 52]. The extra dimension r is interpreted as length scale of the system.

From now on, the capital indices M, N denote the bulk spacetime (r, x^μ) and the greek indices μ, ν denote the boundary spacetime.

2.2 Matching Representations

Once we know the dictionary for the symmetry group, we are able to map Type IIB fields into operators in $\mathcal{N} = 4$ SYM and vice versa. The rule here is that the fields and operators must be the the same representations of SO(2,4)×SO(6) group and SU(N) gauge group[8, 9]. First we notice that the fields on the gravity side must be SU(N) singlet since we can not see stack of branes in the spacetime perspective. The gauge invariant operators on CFT side are denoted by $\mathrm{Tr}(\varphi_1 \dots \varphi_k)$ where φ_i are the operators in SYM and 'Tr' denotes the trace over SU(N) colour indices[7, 8]. I will consider the simplest single trace operator namely $O_l^{i_1 \dots i_l} \equiv \mathrm{Tr}(X^{\{i_1} \dots X^{i_l\}})$ where i is the R-symmetry index labelling the scalar field X^i [9]. We say that this $O_l^{i_1 \dots i_l}$ has a scaling dimension $[O] = l$ since $O \to \lambda^l O$ under the transformation $x^\mu \to \lambda x^\mu$.

This simplest single trace operator is assumed to be dual to a scalar field in the gravity side since they both are singlet representations of the Poincaré group. To be more quantitative, we consider the harmonic expansion of the scalar field in $AdS_5 \times S^5$ background [7, 8]

$$\Phi(x, y) \quad = \quad \sum_l \Phi_l(x)\, Y^l(y) \tag{2.8}$$

Here, $Y^l(y) = c_{i_1 \dots i_l} y^{i_1} \dots y^{i_l}$ are the spherical harmonic function of S^5 and the $c_{i_1 \dots i_l}$ is the symmetric traceless tensor of rank l. In this section, $x = (r, x^\mu)$ and y denote the coordinates on AdS_5 and S^5 respectively. Now we can see that both $y^{i_1} \dots y^{i_l}$ and $O_l^{i_1 \dots i_l}$ are the symmetric traceless representation of the R-symmetry SO(6) and have the scaling dimension $[O] = [Y^l] = l$. This indicates that we made the right assumption. In order to see the role of the scaling dimension in the gravity side, we plug in $\Phi(x, y)$ into the $AdS_5 \times S^5$ Klein-Gordon equation i.e.

$$\Box \Phi(x, y) = \sum_l \Big(\Box\, \Phi_l(x) Y^l(y) \Big) = 0 \tag{2.9}$$

Let us consider a term with $l = \Delta$ in the $\Phi(x, y)$ expansion. We can obtain the mass term for the field $\Phi_\Delta(x)$ by compactify the S^5 subspace. In this case, the Klein-Gordon equation becomes

$$\Big(\Box^{(AdS)} - m_\Delta^2 \Big) \Phi_\Delta(x) \; ; \qquad m_\Delta^2 L^2 = \Delta(\Delta - 4) \tag{2.10}$$

where $\Box^{(AdS)}$ is the Laplacian operator in AdS_5. The more complicated representations can also be matched using similar procedures [8, 9] and two more rules are added to our dictionary.

Bosonic/Fermionic gauge invariant operators	$\Leftrightarrow$	Bosonic/Fermionic fields
Bosonic scaling dimension Δ	$\Leftrightarrow$	mass as a function of Δ

Note that we can add the source to our CFT by including an extra term like $\int O\, \phi_0$ to the action. The brane perspective in FIGURE 1.4 tells us that the open string that lives near the branes is sourced by the ingoing closed string **far away** from the branes. Since the open string mode corresponds the the operator $O(x^\mu)$, the source $\phi_0(x^\mu)$ should be associated to the supergravity field $\Phi(r, x^\mu)$. Since the distance from the brane is $u = L^2/r$, we might guess that $\Phi(r = 0, x^\mu)$ is associated to the source $\phi(x^\mu)$. This is almost right but we need to remember that the spacetime

in the gravity side is no longer $AdS_5 \times S^5$ when L^2/r is too large. We need to put a short distance cutoff at $r = \epsilon$ to guarantee that the ingoing string is not too far away.

Source $\phi(x^\mu)$ of the operator $O(x^\mu)$ living on the branes	$\Leftrightarrow$	Ingoing supergravity field $\Phi(r, x^\mu)$ located at $r = \epsilon \to 0$

2.3 Perturbation & response function

From now on, the discussions will depart from the top-down formalism. Supersymmetry will be dropped and the sphere S^5 will be ignored. In this section, we study how to extract basic physical quantities from the semiclassical theory of gravity in an asymptotic AdS_5 spacetime[1], which is believed to be dual to the conformal field theory of quantum critical point. The gravity side will be referred to as **bulk** and the field theory side will be referred to as **boundary**. These abbreviation came from the fact that the sources of the CFT operators are associated to $\Phi(\epsilon, x^\mu)$ and, intuitively, the current O flows from the spacetime point we inject the source. Since we take $r = \epsilon \to 0$ to be the boundary of the AdS, we may think that the CFT lives on the boundary of AdS [50] although it is not a direct implication from the decoupling argument. Note that, I only discuss about the scalar field here for the concreteness. The similar but a bit more complicated analysis for the fermions can be found in the Appendix A.

We should start by extracting the most basic physical quantities in the field theories which are correlation functions. From the field theory side, we can obtain the 1-point function, for example, from the partition function by taking the functional derivative

$$\langle O(t_E, \mathbf{x})\rangle = \frac{1}{Z[0]} \frac{\delta \ln \mathcal{Z}[\phi_0]}{\delta \phi_0(x^\mu)}\bigg|_{\phi_0=0} \; ; \; \mathcal{Z}[\phi_0] = \left\langle \exp\left[\int d^4x \, O\phi_0\right]\right\rangle_{\text{CFT}} \tag{2.11}$$

where d^4x is the volume element in $\mathbb{R}^4$. The correlation functions obtained from this formalism are the function of the Euclidean time $t_E = it$. The Euclidean time formalism is using here since it gives the weight in the path integral, e^{iS}, the same interpretation as the Boltzmann factor, $e^{-\beta\mathcal{H}}$. The real-time correlation function can be obtained by do the analytic continuation back to the real time.

First of all, for the gravity side and field theory side to gives the same physics through the correlation functions, We need the generating function from the CFT side and the partition function from the gravity side to be equal [2, 8, 9, 30, 50].

$$\left\langle \exp\left[\int d^4x \, O\phi_0\right]\right\rangle_{\text{CFT}} = e^{-S_E[\Phi(r,t_E,\mathbf{x})]} \tag{2.12}$$

This is the famous GKPW formula[2] that allows us to extract physical quantities without even know the explicit form of the CFT action. The right hand side came from the saddle point approximation as the weight e^{-S_E} from the classical gravity configuration dominates. This is

[1] Note that duality still holds for $AdS_4 \times S^7$ [9]
[2] stands for Gubser - Klebanov - Polyakov - Witten

the benefit of taking the large 't Hooft coupling limit $\lambda \to \infty$. The action on the gravity side $S_E[\Phi]$ is Einstein-Hilbert action plus the action of scalar field in the Euclidean time [30]

$$S_E = \int d^{d+1}x\sqrt{|g|}\left[\frac{1}{2\kappa^2}\left(\mathcal{R}+\frac{d(d-1)}{L^2}\right)+\frac{1}{2}(\nabla\Phi)^2-\frac{1}{2}m^2\Phi^2\right] \tag{2.13}$$

evaluated at its extremum with the ingoing boundary condition on Φ. The equation of motion we have to solve is [50]

$$\left[r^2k^2 - r^5\partial_r(r^{-3}\partial_r) + m^2L^2\right]\Phi(r,k) = 0 \tag{2.14}$$

given that $\Phi(r,k) \equiv \Phi(r,\omega_E,\mathbf{k})$ is the Fourier transform of $\Phi(r,t_E,\mathbf{x})$. However, we cannot simply varying the action and naively solve the equation of motion due to the fact that AdS space has a boundary. The following are the conditions we have to impose.

- **Dirichlet boundary condition** : An additional boundary action $S^{(1)}_{\text{bnd}}$ need to be added so that the variational principle is well-define [30, 50, 53]. Without this term, we will not be able to get the equation of motion from varying the action.
- **Ingoing boundary condition** : This condition state that there is no stuff coming out of the Poncaré horizon at $r \to \infty$. In the case of scalar field, this means that we pick only the solution $\Phi(r,t) \sim e^{-i(\omega t - kr)}$ near the boundary [8]. This solution implies that the "wavefront of the field Φ" moves to larger r as t grows [50].
- **Finiteness condition** : There two types of solutions of the equation (2.14) namely **non-normalisable** and **normalisable** modes. As $\epsilon \to 0$, the contributions of the non-normalisable modes lead to the divergence in the on-shell action [50]. This is the usual UV divergence in field theory and can be removed by adding the counter terms $S^{(2)}_{\text{bnd}}$ living at $r = \epsilon$. These counter terms are required to keep $S_{\text{gravity}} < \infty$ and ensure that the field Φ is able to propagate [50, 54, 55]

For example, the boundary terms for the pure AdS (means without any other field) is[3]

$$S_{\text{bnd}} = \frac{1}{\kappa^2}\int_{r=\epsilon} d^4x\sqrt{|\gamma|}\left(\gamma^{\mu\nu}\nabla_\mu n_\nu + \frac{3}{L}\right)$$

where $\gamma_{\mu\nu}$ is the induced metric on the boundary $r = \epsilon$ and n^M is an outward unit vector normal to the boundary. In the **probe limit**, where the field does not back react the spacetime, The scalar field is found to have the asymptotic form [2, 30, 50, 56]

$$\Phi(r,k) = \left(\frac{r}{L}\right)^{4-\Delta}\phi_0(k) + \left(\frac{r}{L}\right)^{\Delta}\phi_1(k) + \dots \quad \text{as} \quad r \ll L \tag{2.15}$$

where Δ satisfy the relation $\Delta(\Delta-4) = m^2$. Here, I shamelessly write down the coefficient of $(r/L)^{4-\Delta}$ as the source $\phi_0(k)$, due to several reasons. First of all, the first term in (2.15) is a **non-normalisable mode** define earlier. This mode costs infinite amount of energy to propagates so it has no dynamics and should be fixed as the source field. Moreover, the scaling

[3] This term is often called the Gibbons-Hawking term [50]

dimension of ϕ_0 is also the same the source in (2.12). This is because $\Phi(r,k)$ is scale invariant under $r \to \lambda r$ as there is no global conformal symmetry on the gravity side. Therefore, $\phi_0(k)$ is scaled as $\phi_0 \to \lambda^{\Delta-4}\phi_0$ [30]. We finally obtain

Source $\phi(t_E, \mathbf{x})$ of the operator $O(t_E, \mathbf{x})$ living on the branes	$\Leftrightarrow$	coefficient ϕ_0 in the solution of Φ $\phi_0(t_E, \mathbf{x}) = (\epsilon/L)^{\Delta-4}\Phi(\epsilon, t_E, \mathbf{x})$

On the other hand, a mode that is allowed to propagate is called **normalisable mode**, which is the second term in (2.15). With this identification, we can write the one point function for any d-dimensional boundary as

$$\langle O(t_E, \mathbf{x})\rangle = -\frac{\delta}{\delta\phi_0} S_{\text{gravity}}[\phi_0]\Big|_{\phi_o \to 0} = -\lim_{r\to 0} \quad r^{d-\Delta}\Pi_E(r, t_E, \mathbf{x}) \tag{2.16}$$

where $\Pi_E(r,k)$ is the canonical momentum defined as $\delta S_E[\Phi]/\delta\Phi(r,k)$. The 1-point function $\langle O\rangle$ is essentially the **response** of the system to the external perturbation at the boundary, $\delta S = \int_{r=\epsilon} O\phi_0$. To evaluate this response, we plug in the solution (2.15) into S_{gravity} and find that it is diverged. Using prescriptions in [50, 56], we found that [30]

$$S_{\text{bnd}}[\Phi] = \begin{cases} \frac{d-\Delta}{2L}\int_{r=\epsilon} d^d x\sqrt{|\gamma|}\Phi^2 & \text{if } d-\Delta < \Delta \\ -\int_{r=\epsilon} d^d x\sqrt{|\gamma|}\left(\Phi n^M \nabla_M \Phi + \frac{\Delta}{2L}\Phi^2\right) & \text{if } d/2 \geq \Delta \geq (d-2)/2 \end{cases} \tag{2.17}$$

In any allowed range of Δ, the 1-point function can be evaluated by using (2.16)

$$\langle O\rangle \quad = \quad \frac{2\Delta - d}{L}\phi_1 \tag{2.18}$$

There is a small caveat when we choose the value of Δ. First of all, we can see that when $\Delta > 4$, the field $\Phi(r,k)$ diverges in the UV i.e. when $r \to 0$. Turning on the operator dual to this field will destroy the asymptotic AdS region of the spacetime and therefore not allowed. The operator O dual to Φ is said to be **irrelevant** since it becomes less important in the IR region. On the other hand, we are allowed to turn on the operator with $\Delta \leq 4$ so that both components in $\Phi_k(r)$ do not diverge at $r \to 0$ and the metric of AdS boundary remains unchanged. The deformation with $\Delta < 4$ is **relevant** as it grows in the large r limit while the one with $\Delta = 4$ is called **marginal**. We may see that this gives $m^2 \leq 0$ but the negative mass does not signal the instability as long as it does not violate the BF bound i.e. $\Delta > (d-2)/2$ (sometimes called the unitary bound) [30, 50].

Now, we can move on to the 2-point function. Instead of giving just the definition. I will try to give some intuition about this 2-point function. For a regular QFT (not necessary the one we just discussed), adding a source term $\int d^d x\, O(x)\delta\phi_0(x)$, means we "kick" the system with a source $\delta\phi_0$. The response $\delta\langle O\rangle$ is found to be [30, 53, 57]

$$\delta\langle O(\omega_E, \mathbf{k})\rangle \quad = \quad \lim_{\delta\phi_0 \to 0} G^E(\omega_E, \mathbf{k})\ \delta\phi_0(\omega_E, \mathbf{k}) \tag{2.19}$$

where $O(\omega_E, \mathbf{k})$ is the Fourier transform of $O(t_E, \mathbf{x})$. The Euclidean Green function $G^E(\omega_E, \mathbf{k})$ is defined as a Fourier transform of

$$G^E(t_E, \mathbf{x}) \quad = \quad \langle T_E O(t_E, \mathbf{x}) O(0, \mathbf{0}) \rangle \tag{2.20}$$

where T_E denotes the Euclidean time ordering. If $\langle O \rangle \to 0$ as $\phi_0 \to 0$ and $\langle O \rangle$ remains small, we can drop δ from $\delta\langle O \rangle$ and write (2.19) as

$$\langle O(\omega_E, \mathbf{k}) \rangle \quad = \quad \lim_{\phi_0 \to 0} G^E(\omega_E, \mathbf{k})\, \phi_0(\omega_E, \mathbf{k}) \tag{2.21}$$

Then compare the 1-point function in (2.19) and (2.18), we will see that the Euclidean Green function can be written as

$$G^E(\omega_E, \mathbf{k}) = -\lim_{r \to 0} r^{2(d-\Delta)} \frac{\Pi_E(r, \omega_E, \mathbf{k})}{\Phi(r, \omega_E, \mathbf{k})} = \frac{2\Delta - d}{L} \frac{\phi_1}{\phi_0} \tag{2.22}$$

After solving the equation of motion one obtain ϕ_0 and ϕ_1, we find that the $G^E(t, \mathbf{x}) \sim (t^2 + |\mathbf{x}|^2)^{-\Delta}$ [2, 8]. This form Green function is exactly the same as the one we obtain from the conformal scalar field theory [10].

Why do we care about this Green function? Let's imagine when we kick a system, a piece of metal for example, with an electric field. The system will generate a response, which is an electric current. This is, in fact, the more general form of Ohm's law.

$$\langle \mathbf{J} \rangle = \sigma \mathbf{E} \tag{2.23}$$

The current $\langle \mathbf{J} \rangle$ is analogous to our response $\langle O \rangle$ and the source $\mathbf{E}$ is analogous to the source ϕ_0. We now see that the conductivity can be extracted almost directly from the Green function. The other transport coefficients such as shear viscosity can also be extracted from the field theory using similar methods [2, 30, 50].

If we want to study the real-time response function instead of the thermodynamic (which is the Euclidean time formalism discussed above). The following are the recipe from [53] to do the analytic continuation back to the realtime

$$\tau \to it \quad ; \quad \omega_E \to -i\omega \quad ; \quad S_E \to -iS \tag{2.24}$$

and the key recipe to obtain the retarded Green function.

$$G^R(\omega, \mathbf{k}) \quad = \quad G^E(\omega_E, \mathbf{k})\Big|_{-i(\omega + i\epsilon)} \tag{2.25}$$

Here, the definition for the retarded Green function is $G^R(t, \mathbf{x}) = i\Theta(t)\langle [O(t, \mathbf{x}), O(0, \mathbf{0})] \rangle$ where $\Theta(t)$ is the step function. The Green functions G^R and G^E can be used to find more complicated transport properties other than viscosity and conductivity. See more details in [30, 57, 58].

2.4 Finite temperature

In the standard field theory approach, the way to study the field theory at finite temperature is to use the Euclidean time formalism. It is due to the close relationship between quantum mechanics and thermodynamics partition function namely

$$\mathcal{Z}_{\text{quantum}} = \langle 0|\, e^{iT\hat{\mathcal{H}}/\hbar}\, |0\rangle \quad ; \quad \mathcal{Z}_{\text{thermal}} = \sum_{\text{all config}} e^{-\beta E} \tag{2.26}$$

The thermal field theory can be formulated by changing $t \to i\tau$ and the topology of our space from $\mathbb{R}^{d+1}$ to $\mathbb{R}^d \times S^1$. Here, S^1 is called the **thermal cycle** with the period $\beta = 1/k_B T$. The behaviour at different temperature can be studied by varying the size of this thermal cycle [16, 25]. The "motion" of a particle in the Euclidean time with a finite size thermal cycle is illustrated in FIGURE 2.2.

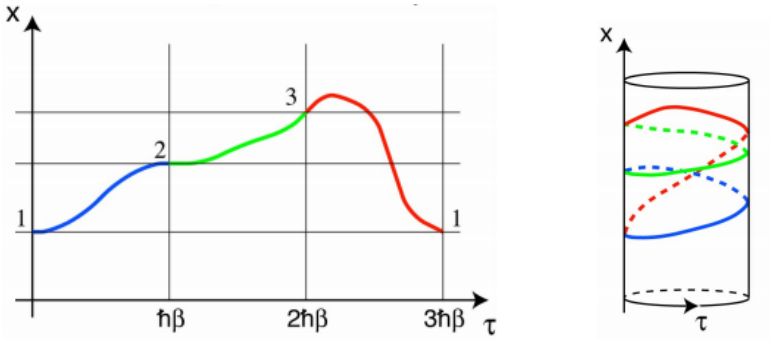

FIGURE 2.2: **LEFT**: A world line of a particle travelling from $\tau = 0 \to 3\beta$ which is equivalent to the world line wrapping on the cylinder of diameter β (**RIGHT**). These two figures are taken from [25]

In order to study the real-time correlation functions, we can do the analytic continuation from the Euclidean correlation functions as outlined in the previous section. However, by doing that, we simply lose the information about temperature. The standard way to include the temperature is to change the definition of the expectation value from averaging over the pure quantum state to mixed states. This redefinition can be written as

$$\langle O_1(t_1)O_2(t_2)\ldots\rangle \quad \equiv \quad \sum_\lambda \langle\lambda|e^{-\beta\bar{H}}O_1(t_1)O_2(t_2)\ldots|\lambda\rangle$$

where $\mathbb{1} = \sum_\lambda |\lambda\rangle\langle\lambda|$ and $e^{-\beta\bar{H}}$ is the density matrix operator [16]. The operator $\hat{H}$ is the Hamiltonian of the system. This approach works very well when the Hamiltonian $\hat{H}$ is diagonalisable i.e. it can be written as $\hat{H} = \sum_i E_i \hat{a}^\dagger \hat{a} + \text{const}$. However, this method does not work in the strongly correlated systems such as conformal field theory, where the Hamiltonian is not diagonalisable [33].

It turns out that approaching the problem using the holographic principle provides an elegant way to deal with the field theory at finite temperature temperature. Since the temperature is encoded in the size of thermal cycle, we need the spacetime in the bulk which is periodic in τ

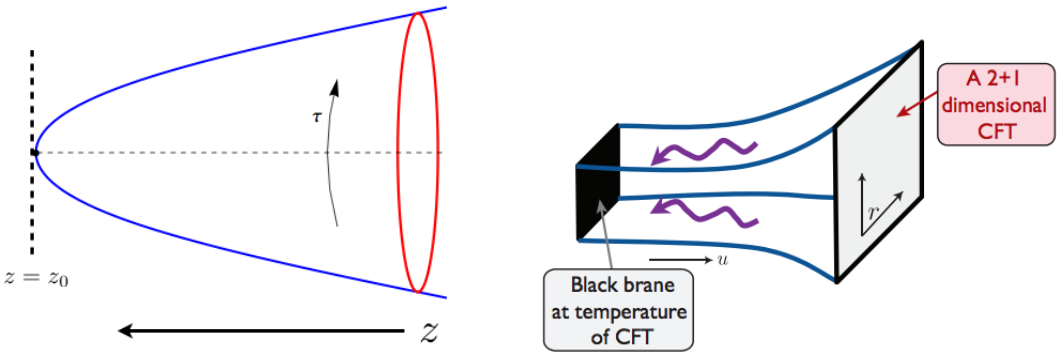

FIGURE 2.3: **LEFT**: The Euclidean AdS Schwarzschild solution, the thermal cycle S^1 smoothly shrink as $r \to r_0$ **RIGHT** The real time version of the metric on the LEFT. The hyperspace at r_0 becomes a black brane i.e. black hole with a flat topology.These two figures are taken from[2] and [33]

direction. The periodicity in τ implies that $\frac{\partial}{\partial \tau}$ is the Killing vector. Once we take into account the translation symmetry $\mathbf{x} \to \mathbf{x} + \mathbf{c}$, the Birkhoff's theorem indicates that there is only one metric solution with all the symmetries i.e.

$$ds^2 = \frac{L^2}{r^2}\left(f(r)d\tau^2 + f(r)^{-1}dr^2 + dx^i dx^i\right) \quad ; \quad f(r) = 1 - \left(\frac{r}{r_0}\right)^d \tag{2.27}$$

for d-dimensional boundary theory. This solution is referred to as "*AdS* **Schwarzschild solution**". In the Appendix B, I show that this solution indeed satisfies the Einstein-Hilbert action with the negative cosmological constant and τ has a period $4\pi r_0/d$. The real time can be obtained from $\tau \to it$. We see that, as $g_{tt}(r_0) = 0$, the hyper surface $r = r_0$ is infinitely redshifted with respect to the observer at the boundary. This is the definition of the black hole despite the fact that the object at $r = r_0$ has a topology of a plane depicted in FIGURE 2.3(**RIGHT**). The temperature can be varied simply by sliding the **black brane** along the $r-$direction as $kT \propto 1/r_0$. As $r_0 \to \infty$, the black brane becomes the Poincaré horizon and we are back to the conformal field theory at $T = 0$.

Temperature T of the field theory $\quad \Leftrightarrow \quad$ "Black brane" at $r_0 = d/4\pi k_B T$ in the bulk

By introducing the temperature, we can then study the thermodynamics of this system from the free energy $F = -kT \ln \mathcal{Z}$. One of the most remarkable features is that, the entropy calculated from the statistical physics formula

$$S = -\frac{\partial F}{\partial T} = \frac{(4\pi)^d L^{d-1}}{2\kappa^2 d^{d-1}} V_{d-1} T^{d-1} \tag{2.28}$$

is scaled with the spatial volume V_{d-1} of the boundary. This spatial volume can be thought of as an "Area" in d spatial dimensions. The entropy calculated this way is essentially the same as calculating the area of the horizon and put into the Bekenstein-Hawking entropy $S = 8\pi A_{\text{horizon}}/\kappa^2$. This makes the holographic duality very peculiar since we will be obtain the entropy of the field theory without actually evaluating the partition function. It is hard to prove whether the entropy evaluated using Bekenstein-Hawking formula is actually equal to the

entropy of the field theory or not since the calculation on the field theory side is terribly difficult[4]. Although, there are not many supporting evidences, we still assume that the below statement is true.

Entropy of the field theory $\Leftrightarrow$ Black Hole entropy stored by the horizon

Using similar methods, the other thermodynamics quantities, such as heat capacity, can also be extracted from the free energy F[2, 30]. We can then compare these quantities with the experimental results to check whether our bottom-up model works or not.

This black brane solution also offers a lot easier way to study the real time response of the system. In the case of scalar field, for example, we just have to solve for e.g. ϕ_0 and ϕ_1 in this bulk instead of AdS_{d+1}. We also need to specify the asymptotic boundary condition near the horizon which the detail can be found in [53]. We now see that the problem of diagonalising the Hamiltonian, which may not doable, boils down into the problem of solving differential equations. Note, we are unable to probe the physics in the interior deeper than r_0 since it is blocked by the event horizon. This agrees with the fact that the thermal fluctuation creates noises, which destroy our ability to probe the energy lower much lower than $k_B T$

We may also think of this black brane as a natural heat bath that heat up the boundary CFT by the Hawking radiation. Note that, the scale r_0 set by the position of the black brane breaks the scale invariant of the field theory. This may deviate from the original top-down set up but it is ok as long as the boundary $r \to 0$ remains asymptotic AdS.

2.5 Finite Density

The finite density is normally referred to as "internal symmetry" in a standard field theory course. It is because the conserved charge $\int dV_{d-1} J^t$ is the number of particles, where J^μ is the Noether current associated to the U(1) global symmetry. The finite density effect can be manifested by adding the source term $\int d^d x\ J^\mu A_\mu$ and the Lagrange multiplider $\int d^d x\ \Lambda \partial_\mu J^\mu$, which leads to the constraint $\partial_\mu J^\mu = 0$. This second term can be absorbed in the source A_μ by demanding that A_μ transforms as $A_\mu \to A_\mu + \partial_\mu \Lambda$. According to our dictionary rules, the source term A_μ at the boundary becomes the classical field in the bulk. The freedom of choosing the Lagrange multiplier, Λ, turns into the U(1) gauge symmetry.

The internal U(1) symmetry at the boundary $\Leftrightarrow$ U(1) gauge field in the bulk

The action of the fields in the bulk has to includes the Mexwell term. This Einstein-Maxwell action in the Lorentzian signature has the form [21]

$$S_{EM} = \int d^{d+1}x \sqrt{|g|} \left[\frac{1}{2\kappa^2} \left(\mathcal{R} + \frac{d(d-1)}{L^2} \right) + \frac{1}{4q^2} F_{MN} F^{MN} \right] + S_{\text{bnd}} \tag{2.29}$$

[4]Nevertheless, there is a famous field theory setup called D1-D5-P system that the entropy calculated from field theory side and gravity side are equal [59]

In the equilibrium thermal system, there are two components of the gauge field we can turn on namely

$$A \quad = \quad A_t(r)dt + B(r)x\,dy \tag{2.30}$$

The non-zero $A_t(r=\epsilon)$ is resulting the extra boundary term $\int d^dx J^t A_t$, which is equivalent to adding the chemical potential to the boundary field theory. The language of the chemical potential might be a bit unusual for non-condensed matter people but, actually, we have seen a term like this in the complex scalar field theory. The chemical potential term plays the role of a mass^2 i.e it is the term like $\int d^dx\ \mu\ (\varphi^\star\varphi)$. The term $\varphi^\star\varphi$, which is the J^t component of the Noether current, plays the role of the local number density. By comparing the action at the boundary in both pictures, we can identify that

$$\mu = A_t(r=\epsilon) \quad ; \quad \langle J^t\rangle = F^{rt}(z=\epsilon) \tag{2.31}$$

Similarly, the term $B(r=\epsilon)$ can be identified as a magnetic field [30] but I will turn it off for the rest of this dissertation.

There is a subtlett I have to mention here. Although, the term $\int d^dx\ J^\mu A_\mu$ is acting as a source, it is different from $\int d^dx\ O\phi_0$ in the previous discussion. The source ϕ_0 acts as a probe that generates the small response $\langle O\rangle$ with no backreaction to the spacetime. However, the source A_μ is a gauge field in the bulk generated from the electrically/magnetically charged objects in the bulk. The expectation value $\langle J^t\rangle$ and $\langle B\rangle$ can be arbitrarily large depending on the amount of charges in the interior of the asymptotic AdS spacetime.

The charged matter can be either hidden behind the black brane horizon or floating in the bulk [33, 52] (or both [60]). In either cases, the space times are no longer AdS_4. In this chapter, I will focus on the first case where the black brane itself is the source of all the electric field.

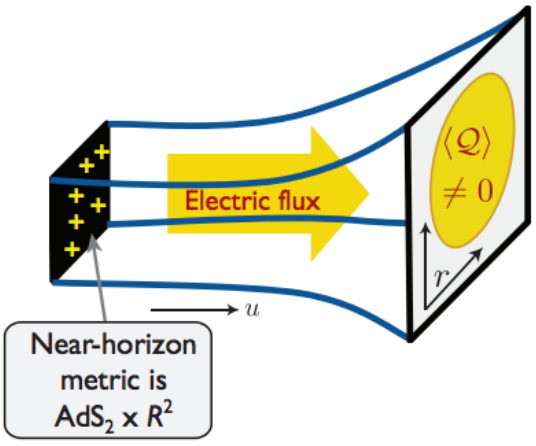

FIGURE 2.4: The AdS Reissner-Nordstrőm (AdS RN) black brane acts as both source of temperature and charge. The electric flux from the black brane propagate through the bulk and induce the charge at the boundary. Note that, at $T = 0$K, the geometry in the IR region becomes $AdS_2 \times \mathbb{R}^2$ while the UV region remains AdS_4. The figure is taken from [33]

In order to extract the physical quantities, we need to look at the equation of motion derived from the Einstein-Maxwell action. With an appropriate boundary terms, the equation of motions

looks like the following.

$$\mathcal{R}_{MN} - \frac{1}{2}g_{MN}\mathcal{R} - \frac{d(d-1)}{L^2}g_{MN} = \frac{\kappa^2}{q^2}\left(2g^{PQ}F_{MP}F_{NQ} - \frac{1}{4}g_{MN}F_{PQ}F^{PQ}\right) \quad (2.32)$$

$$\nabla_M F^{MN} = 0 \quad (2.33)$$

The solution of these equations that gives the nonzero $A_t(\epsilon)$ and asymptotic AdS boundary is the charged black brane solution or the "AdS **Reissner-Nordstrőm (AdS RN) solution**" [21].

$$ds^2 = \frac{L^2}{r^2}\left(-f(r)dt^2 + dx^i dx^i + \frac{dr^2}{f(r)}\right) \quad (2.34)$$

with

$$A_t = \mu\left(1 - \left(\frac{r}{r_0}\right)^{d-2}\right); \qquad f(r) = 1 - \left(\frac{r}{r_0}\right)^d + \frac{(d-1)\kappa^2\mu^2(r^{d-2} - r_0^{d-2})}{(d-1)q^2L^2r_0^{2d-2}} \quad (2.35)$$

We can work out the temperature using the thermal cycle method and obtain

$$T = \frac{d}{4\pi r_0}\left(1 - \frac{(d-2)^2}{d(d-1)}\frac{\kappa^2\mu^2r_0^2}{q^2L^2}\right) \equiv \frac{d}{4\pi r_0}\left(1 - \frac{r_0^{2d-2}}{r_*^{2d-2}}\right) \quad (2.36)$$

We see that the temperature no longer depends only on a single length scale r_0 but also the other scale r_* sets by $\kappa\mu/qL$. We observe that if $r_0 \ll r_*$ i.e. $k_BT \gg \mu$, the metric returns to the AdS Schwarzschild and the spacetime contains a naked singularity when $r_0 > r_*$ [21]. The most interesting situation is when $r_0 \to r_*$ since it is dual to the finite density field theory at a low temperature, where the quantum effect dominates.

Let's consider the region near the horizon $r_0 = r_*$. We found that $f(r)$ has a double zero as $r \to r_0$ that is $f(r \to r_0) \approx (r_0 - r)^2 + \ldots$. Consequently, the near-horizon metric can be repackaged into $AdS_2 \times \mathbb{R}^{d-1}$ [21]

$$ds^2 = \frac{L_2^2}{\zeta^2}(-dt^2 + d\zeta^2) + \frac{L^2}{r_*^2}dx^i dx^i\,; \quad A_t = \frac{qL_2}{\kappa\zeta} \quad (2.37)$$

where

$$\zeta \equiv \frac{r_*^2}{d(d-1)(r_* - r)}; \quad L_2 \equiv \frac{L}{\sqrt{d(d-1)}}$$

We can see that, the "area" of the horizon is non-zero even at the zero temperature due to the $\mathbb{R}^2$ subspace. We know from our previous dictionary rule that the area of the horizon is proportional to the thermal entropy of the boundary theory. This means that the ground state has non-zero entropy at zero temperature and hence degenerated. In the absence of the supersymmetry or others symmetries to protect this degeneracy, this state is believed to be an intermediate state that gives rise to the other exotic states such as non-Fermi liquid, superconductor, insulator etc. as depicted in FIGURE 2.5 [61].

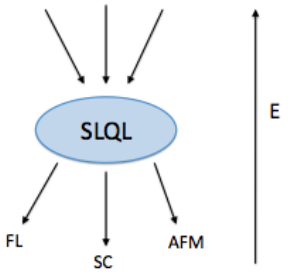

FIGURE 2.5: The illustration of of the RG flows from the SLQL to the other exotic states [61]
.

This $AdS_2 \times \mathbb{R}^{d-1}$, or sometimes called **semi-local quantum liquid** (SLQL) [61, 62], is actually a key player in the game of applied AdS/CFT. The first AdS/condensed matter application [39] use almost the same bulk theory as we discussed above, but with the magnetic charge added to the black brane. If we put a charge bosonrs to the bulk, we find the superconductor phenomena [63–65]. If we put the charge spinor in the bulk we find the fermi surface [66–68]. The fact that the theory of spinors in the bulk is dual the strongly interact spinors (fermions) in the boundary, gives hope that we might be able bypass the sign-problem brick wall and get our hand on the non-Fermi liquid theory!

I would like to present one of landmark of the holographic principle achieved by the studies of AdS RN. The optical conductivity can be obtained by considering the response from the small electric field in the boundary direction such that 1-form gauge field becomes $A = (A_t, \delta A_x, 0, 0)$ [30]. In FIGURE 2.6, the optical conductivity of AdS RN is presented and compared with the results from graphene experiment [69]. The two results are strikingly similar. Further studies of the holographic models with broken translational symmetry [70–73] also found the peak of the real part of the optical conductivity at small ω (Drude peak) that is not visible in the AdS RN result.

The tutorial on calculating the optical conductivity can be found in [30]. The full mathematica code that is used to obtain the plot on the LHS of FIGURE 2.6 is adapted from the exercise in 2$^{\text{nd}}$ Mathematica summer school in theoretical physics. The exercises and the mathematica notebook can be found in `http://msstp.org/?q=node/254`.

2.6 Geometry and Phase Transition

Let us come back to the story of $\mathcal{N} = 4$ SYM and the type IIB supergravity again to discuss the role of the black hole event horizon in the story of the phase transition.

Prior to the discovery of the AdS/CFT, Hawking and Page [74] found the black hole phase transition in the global AdS space (defined in Section 2.1). It can be shown that the boundary of the global AdS_{p+2} can be confomally mapped into half of the manifold $\mathbb{R} \times S^p$ [8] as shown in FIGURE 2.7. Here $\mathbb{R}$ represent the time direction. We can do the analytic continuation from

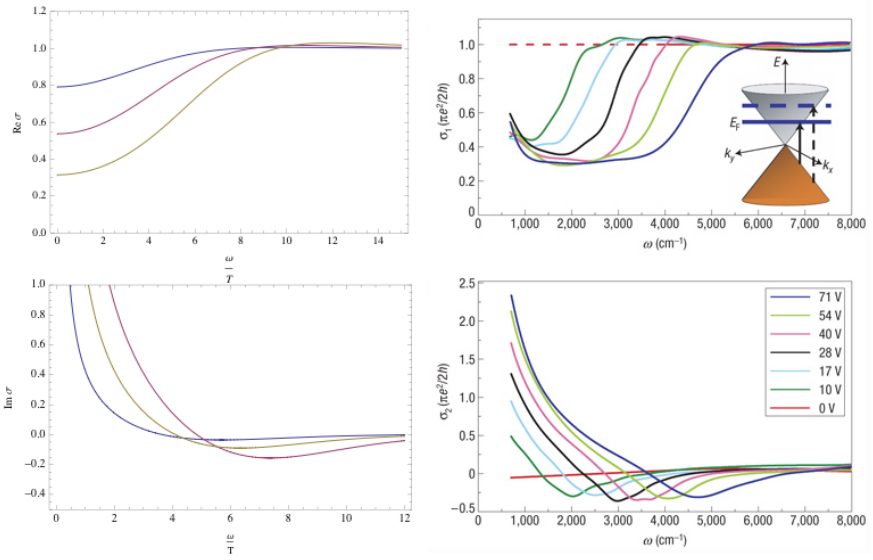

FIGURE 2.6: The caparison between the optical conductivity from AdS/CFT (**LEFT**) and the grapheme experiment (**RIGHT**). The top two figures represents the real part of the conductivity while the bottom two represent the imaginary part. Different colours on the AdS/CFT results denote different value of the chemical potential μ. The colours on experimental results denote values of gate voltage, which plays the role of chemical potential [69] .

the real time to the Euclidean time. The time domain $\mathbb{R}$ is compactify into a thermal cycle. Hence, the boundary of the Penrose diagram can be conformally mapped inbto $S^1 \times S^p$

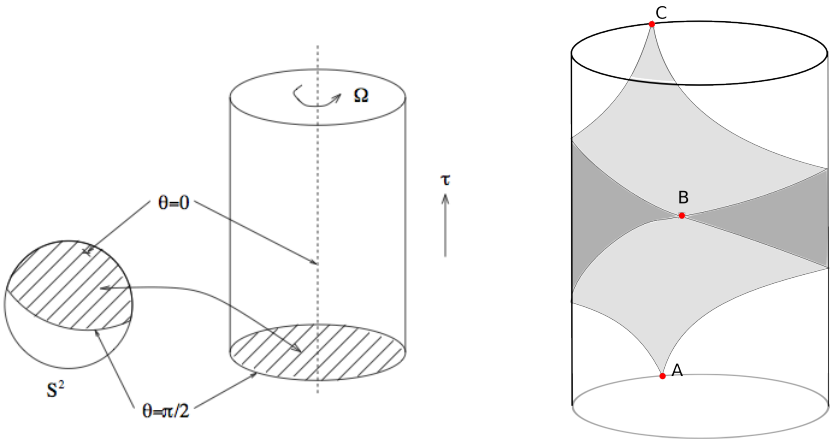

FIGURE 2.7: **LEFT :** The map between global AdS_3 and $\mathbb{R} \times S^2$. The shaded face of the cylinder is mapped into half of the sphere S^2 [8]. **RIGHT :** The Poincaré patch embedded in the global AdS is represented by the wedgeABC.

It turns out that there are two solutions of the Einstein equation with this boundary condition. Both solutions are shown in FIGURE 2.8. The first solution has a decreasing Euclidean thermal cycle's radius as the radial direction r increases. This is the AdS Schwarzschild solution. The second one is when the sphere S^p is shrinking instead of S^1. We call this solution the **thermal AdS** [7]

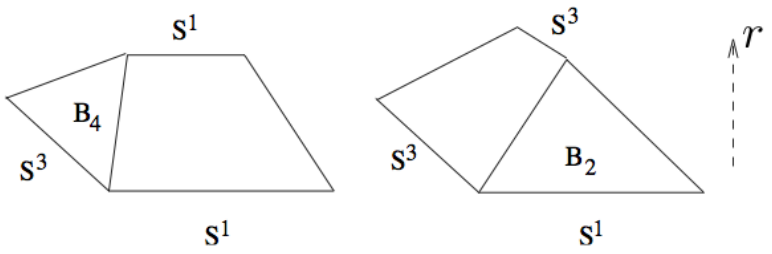

FIGURE 2.8: Evolution of the two solutions along AdS radial direction, r, for $p = 3$. **LEFT :** The thermal AdS solution with the topology $S^1 \times B_4$. **RIGHT :** The AdS Schwarzschild solution with the topology $B_2 \times S^3$. B_n is the n-dimensional ball with the boundary S^{n-1} This figure is taken from [7].

In order to find out which solution is more preferable, one needs to compare the on-shell actions between these two configurations and see which solution gives the smallest action. It turns out that the thermal AdS is more preferable when the temperature (obtained from the thermal cycle's period) is less than $T_c = p/2\pi L$ and vice versa. This thermal phase transition is known as **the Hawking-Page transition**. The mathematical verification of the statement above can be found in [2, 7] or [74] for brave.

It was Witten [75] who pointed out that the global AdS spacetime is dual to the SU(N) $\mathcal{N} = 4$ SYM with a finite volume. The thermal AdS phase is dual to the **confining phase** involving only $SU(N)$ singlets. The AdS Schwarzschild is dual to the **deconfined phases** corresponds to the state with the gauge degree of freedom such as free quarks and gluons. This matching can be shown explicitly by calculating the Wilson loop similar to what we do in the quark confinement case, see e.g. [76]. One can also argue that, in the deconfining phase, the black hole entropy $\sim 1/\kappa^2$ is of order N^2. This means that the degree of freedom of the boundary theory is $\propto N^2$. This N^2 dependence can be obtained from the field theory side by considering the dimensions of SU(N) gauge group. On the other hand, in the confining phase, the black hole in the bulk theory vanishes. This means that the entropy is of order N^0. It is expected that, in the confining phase, the N^2 gauge degree of freedoms combine in a single gauge singlet.

Field theory where all gauged degree of freedom	$\Leftrightarrow$	Gravity theory with confining geometry
confined into the gauge singlet		i.e. no event horizon
Phase transition in the boundary theory	$\Leftrightarrow$	Deformation from one spacetime to the other

Other than the Wilson loop, the Polyakov loop and the entanglement entropy are also proposed to be quantities which can distinguish the confining and deconfined phase [2, 77]. All of these non-local measurements are beautifully realised in the dual gravity theory as certain surfaces in the bulk geometry [77]. I will focus on the entanglement entropy in particular. The proposed holographic prescription for calculating entanglement entropy is the the following. Consider the d-2 dimensional surface Σ dividng the region A and B in d dimensional AdS boundary. The entanglement entropy is proportional to the area of the minimal surface Γ extended in the bulk, given that the surface Γ ends on Σ i.e. $\partial\Gamma = \Sigma$. This statement can be

made more precise by writing the famous Ryu-Takayanagi formula [37].

$$S_E = \frac{A_\Gamma}{4G_N} \tag{2.38}$$

where G_N is the Newton's constant in d+1 dimensions. The illustrations of Σ and Γ are shown in FIGURE 2.9. This nice and simple formula enhances our ability to calculate the entanglement entropy and provides an access to the quantum information aspects of both black hole and condensed matter systems.

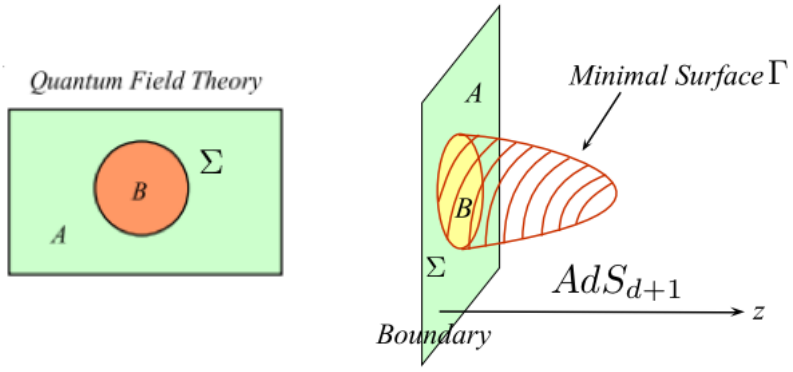

FIGURE 2.9: **LEFT**: The surface Σ separate the region A and B on the *AdS* boundary where the field theory lives. **RIGHT** : The minimal surface Γ extended in the interior of the *AdS* space.These two figures are adapted taken from [78]

So how can we distinguish the confining/deconfined phase using entanglement entropy? Let's consider the case where the hypersurface Σ is the two infinite spatial hyperplane separated by the distance R. The minimal surface Γ in confining and deconfined phase are different as depicted in FIGURE 2.10. The entanglement entropy in the confining phase is proportional to the disconnected hypersurface Γ and takes the form

$$S_E \sim \frac{\text{Vol}(\Sigma)}{\epsilon^{d-2}} + \Big(\text{const} \times \text{Vol}(\Sigma)\Big) \tag{2.39}$$

where $\text{Vol}(\Sigma)$ is the volume of the hypersurface Σ and ϵ is the short distant cutoff [77]. There is no R-dependent term at the leading order in this phase. On the other hand, in the deconfined phase, the entanglement entropy becomes

$$S_E \sim \frac{\text{Vol}(\Sigma)}{\epsilon^{d-2}} + R\Big(\text{const} \times \text{Vol}(\Sigma)\Big) \tag{2.40}$$

The R-dependence in the second term came from the fact that the spacetime has to be smooth near the horizon. Hence, Γ is connected [77]. This R-dependence can be used to distinguish confining and deconfined phase.

So far, we have discussed the recipe to make the theory of gravity that is dual to several field theories. It turns out to be quite simple in the bottom-up approach. We know how to turn on the temperature, finite density, magnetic field and confine or deconfine the SU(N) gauge degree of freedom. Our ability to calculate things is also enhanced by the holographic dictionary. We see that the Green function of the strongly correlated system can be obtained by solving

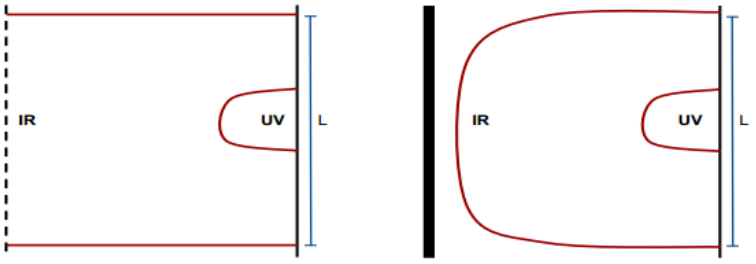

FIGURE 2.10: **LEFT :** The minimal surface Γ in the confining phase where the deep IR geometry is truncated. **RIGHT :** The minimal surface in the deconfined phase. The surface Γ has to be connected since the black brane require the geometry to be smooth at the horizon. These figures are taken from [77].

differential equations instead of calculating many loop-corrections. Moreover, the complicated quantity such as the entanglement entropy is turns out to be the minimal area in asymptotic AdS spacetime.

It is probably a good place to stop giving a general dictionary rules and start to see what can holographic duality tell us about the real systems, especially systems of fermions.

Chapter 3

Holographic (non-)Fermi liquid : models with fermions

In the previous section, we see that the gravity dual provide a powerful way to calculate the retarded Green function of the strongly interacting quantum field theory. It is interesting to know what the Green function looks like if the boundary field theory is a system of strongly correlated fermions.

We know that, from the Pauli exclusion principle, the states of Fermions form a "sphere" in the momentum space. The surface of this sphere at $\mathbf{k} = \mathbf{k}_F$ is called the Fermi surface. Therefore, the Green function should be something like

$$G_R^{-1}(\omega, \mathbf{k} \to k_F) \quad = \quad \omega - v_F|\mathbf{k} - \mathbf{k}_F| + \dots \tag{3.1}$$

where $\mathbf{k}_F \neq 0$ indicates the existence of the Fermi surface. The $(\dots)$ part is the electron's self-energy $\sim \omega^2$ for the Landau-Fermi liquid theory. Hence, for the field theory with Fermi surface(s), the inverse Green function is expected to be zero at some $\mathbf{k} \neq \mathbf{0}$ and $\omega = 0$. This property is easy to see once we obtain the Green function from the gravity side.

Other than the presence of the Fermi surface, the theory of the fermions has to satisfies the **Luttinger count**. In a case of non-interacting Fermi gas, it simply states that the size of Fermi surface k_F is constrained by the number of the fermions $\mathcal{Q}$, namely $\mathcal{Q} \propto k_F^{d-1}$ for a Fermi gas in $d-1$ spatial dimensions. However, it has been proven that this relation remains valid to all orders in the fermion-fermion interaction. We can also have a system with N different fermionic operator ψ_l, each with different global $U(1)_l$ symmetry $\psi_l \to e^{iq_l\theta}\psi_l$. In this configuration, the Luttinger count is generalised into

$$\langle \mathcal{Q} \rangle \quad = \quad \sum_{l=1}^{N} q_l V_l \tag{3.2}$$

where q_l is the U$(1)_l$ charge of the spinor field and V_l is the volume of the Fermi surface in momentum space. The relation remains invariant as long as none of the $U(1)_l$ symmetry is broken [79].

With the holographic principle, we found a nice and elucidative interpretation that the relation is actually the "Gauss law". Recall that the volume of the Fermi surface(s) corresponds number of fermonic states on the boundary. This "Gauss law" is simply stating that the number of the states is equal to the electric flux generated by the charged object(s) in the bulk. This relation can be violated, for example, when the electric flux is generated from behind the horizon and when one of the global $U(1)_l$ symmetry is broken, as I will discuss later.

In this chapter, I will discuss various model which the Fermi surface is found. Firstly, I will summarise the discovery of the non-Fermi liquid zoo in the AdS RN metric and hence explain why this is not the end of the story. Next, I will introduce, probably, the most popular model where the fermions are treated as a fluid in bulk. This model is called the **electron star** due to its similarity to the Tolman-Oppenheimer-Volkov neutron star. We will then move away from the fluid approximation and explore the gravity model with the dilaton and the nice features we can obtain of this model. Finally, I will give an example where the physics of the black hole, system of electrons and entanglement entropy come into the same physical problem.

3.1 Probing $\mathbf{AdS}_2 \times \mathbb{R}^2$ with fermions

The starting assumption is that, we are in the probe limit, which means the probe fermion is unable to signal the backreaction. The charge q in this limit are restricted to be small to avoid the backreaction i.e. $mL \ll 1$ and $q \ll \langle \mathcal{Q} \rangle$. As outlined in Appendix A, the spinor correlation function in the AdS RN background.

$$G_R(\omega, \mathbf{k} \to \mathbf{k}_F) = D(\omega, \mathbf{k}) A^{-1}(\omega, \mathbf{k}) \tag{3.3}$$

where A and D is define is the the solution near AdS_4 boundary i.e. [53]

$$\Psi(r \to 0) \quad = \quad \begin{pmatrix} A r^{\frac{3}{2}-mL} \\ D r^{\frac{3}{2}+mL} \end{pmatrix} + \dots \tag{3.4}$$

In the Appendix A, I showed that the retarded Green function in the $AdS_2 \times \mathbb{R}^2$ has the form

$$\mathcal{G}_k \quad = \quad c(\nu_k)(-i\omega)^{2\nu_k} \tag{3.5}$$

I denote the retarded Green function in $AdS_2 \times \mathbb{R}^2$ as $\mathcal{G}$ to distinguish it from the Green function G in full asymptotic AdS_4 spacetime. The scaling exponent ν_k is defined as

$$\nu_k \quad = \quad \sqrt{\frac{1}{6}\left(m^2 L^2 - \frac{q^2 L^2}{\kappa^2} + k^2 r_*^2\right)} \tag{3.6}$$

By incorporating the region $r \to 0$ and $r \to r_*$, one can show that at small ω the retarded Green function becomes[62]

$$G_R(\omega, \mathbf{k}) = \frac{D_+^{(0)} + \omega D_+^{(1)} + \mathcal{G}_k(\omega)(D_-^0 + \omega D_-^{(1)})}{A_+^{(0)} + \omega A_+^{(1)} + \mathcal{G}_k(\omega)(A_-^0 + \omega A_-^{(1)})} \tag{3.7}$$

However, we know that $\mathcal{G}_k \sim \omega^{2\nu_k}$. Hence, when $G_R^{-1}(\omega = 0, \mathbf{k}_F)$ vanish, we can expand $A_+^{(0)}$ around $\mathbf{k}_F$ and obtain the celebrated formula

$$G_R(\omega \to 0, \mathbf{k} \to \mathbf{k}_F) \simeq \frac{D_+^{(0)}}{|\mathbf{k} - \mathbf{k}_F|\partial_k A_+^{(0)} + \omega D_+^{(1)} + c(\nu_{k_F}) A_-^{(0)} \omega^{2\nu_{k_F}}} \tag{3.8}$$

and hence can be rearranged in to a very peculiar form

$$G_R^{-1} \simeq Z^{-1}\left(-\frac{\omega}{v_F} + |\mathbf{k} - \mathbf{k}_F| - h\omega^{2\nu_{k_F}}\right) \tag{3.9}$$

This form of the Green function is almost the same in the one from Landau-Fermi liquid theory. The difference are that $\Sigma(\omega)$ is no longer restricted to be $\sim \omega^2$. There might also be several Fermionic modes in the bulk that gives the $G_R^{-1} = 0$ but with different values of v_F and k_F. Consequently, this implies that there can be more than one Fermi surface in the boundary theory. Therefore, the Green function of the AdS RN shows us the signature of the non-Fermi liquid! The parameter ν_{k_F} can be tuned by varying free parameters in our gravity theory and we found four different regions namely

(i) $2\nu_{k_F} > 1$: The decay rate $\sim \omega^{2\nu_{k_F}}$ is very small and the field theory is expected to have a long-lived low energy excitation. Note that at $\nu_{k_F} = 1$, we have the usual Landau-Fermi liquid

(ii) $2\nu_{k_F} < 1$: The decay rate diverge and the system represents the fermionic states with no long-lived excitation.

(iii) $2\nu_{k_F} = 1$: This region is called the "marginal Fermi liquid". It turns out that h have poles when ν_{k_F} and v_F simply vanished. These two infinity knock each other off and we are left with

$$G_R^{-1} \simeq Z^{-1}\left(|\mathbf{k} - \mathbf{k}_F| + \tilde{c}_1 \omega \log \omega + c_1 \omega\right) \tag{3.10}$$

This form is exactly the same as the phenomenological model in (1.12)! The detailed calculation toward this form can be seen in Section VI A and Appendix C of [62]

(iv) $\nu_{k_F}^2 < 0$: This region is called the "oscillatory region" [21] . This condition implies that $k_F^2 < r_*^{-1}(q^2L^2/\kappa^2 - m^2L^2)$. For the term $k_0^2 \equiv L^2(q^2/\kappa^2 - m^2) > 0$, one can show that the electric potential is able to produce pairs product of fermion/antifermion in the bulk [80]. This pair product will create the finite density bulk fermions that will backreact the bulk metric.

Although, this model exhibits the Fermi liquid and allows us to obtain classes of non-Fermi liquids, it is not the end of the strongly interacting electrons' story. Firstly, the entropy at zero

temperature is nonzero thermal entropy which may leads to am instability [21]. Secondly, one can test the Luttinger count of this system and finds that the relation is badly violated. This is because only the small portion of the total charge $\langle \mathcal{Q} \rangle$ forms the Fermi surface and a large amount of flux came from the horizon [81]. Finally, in the case where $k_0^2 > 0$, we can read off the size $\mathbf{k}_F$ of the Fermi surfaces at a given q from orange fringes in FIGURE 3.1. One finds that there always exist the Fermi surface(s) in the oscillatory region $\nu_{k_F}^2 < 0$. If there are a finite number of fermions in the bulk, the modes in the oscillatory region are very likely to be occupied and that leads to the instability.

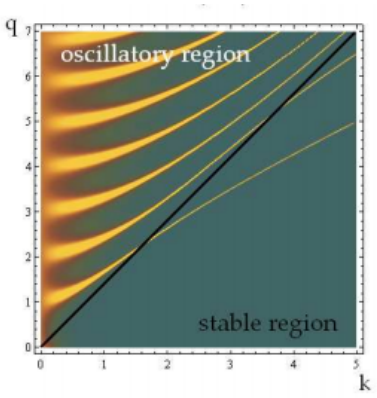

FIGURE 3.1: The spectral density or $\mathrm{Im}G_R(\omega, \mathbf{k})$ as a function of q and k at $\omega = 0$ when $k_0^2 > 0$.The orange fringes indicate the value of q and k where the Green function becomes large. The location of the Fermi surfaces k_F at a fixed q can be read off by look at the intersections between the orange fringes and the line $q =$ constant. We always find the Fermi surface in the oscillatory region for any value of q. This plot is taken from [67]

Let's look at this oscillatory region in a bit more detail and see what we can do when the backreaction is taken into account.

3.2 Fermions pair production and backreacted spacetime

Let us start by looking at the electrostatic potential in the bulk generated by the AdS RN black brane. The electrostatic potential, or sometimes called local chemical potential in $AdS_2 \times \mathbb{R}^2$, is given by [21]

$$\mu_{\text{local}}(r) = \sqrt{g^{tt}} A_t = \frac{|q|}{\kappa} \tag{3.11}$$

If this potential energy is greater than the mass m of the bulk fermion, electron pair production occurs. This condition is exactly the same as $q^2L^2/\kappa^2 - m^2L^2 > 0$ discussed in the previous section. Hence existence of the oscillatory region implies that the pair production is possible.

So, what will happen when there is a pair production in the bulk? It is illustrated by the cartoon in FIGURE 3.2. The negative charged particle will falls back into the black brane and reduces the total charge of the brane. The positive charge will be hovering in the bulk and form a "Fermi surface" of the weakly interacting Fermi gas in the bulk. Eventually, the black brane configuration will no longer be energetically favourable and we are left with fermions in a curved background.

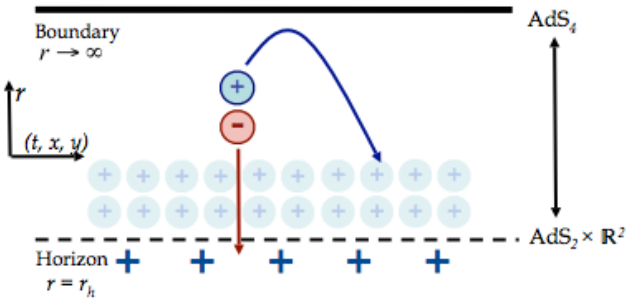

FIGURE 3.2: The cartoon illustrates the pair production. The negative charge falls back to the black brane while the positive charge form a bulk Fermi gas. The radial direction r in this figure is L^2/r in our notation. This plot is taken from [82]

Once the black brane vanishes, we will be back to the many-body fermions problem, which is the problem we are trying to solve. In fact, it is even harder. The fermions interaction is highly non-local since they know about each other's wave function[1] and, as a result, arrange themselves such that they are not in the same state. This non-locality deform the metric in a very complicated way. So one might think that doing the many fermions problem in flat space is probably easier than solving the Einstein equation with non-local interactions.

Fortunately, the analogy between the RG flow and the *AdS* spacetime gives us a hint. Since each value of r corresponds to the energy/length scale in the RG flow language, it does not make sense if the fermions wave function is nonlocal in z. There are two proposed models associated to this local approximation namely

Dirac Hair : By restricting the number of normalisable mode to be one, we can get rid of the non locality in z. The field theory dual to this gravity has only a single Fermi surface [83]. However, the gravitational consistency properties are not fully understood [84].

Electron Star : By putting many fermions in the bulk, one can treat them as a fluid in a similar way as the neutron star. The backreacted gravity solution is known in this case but its dual field theory has infinitely many Fermi surfaces as a result [85–87].

I will review about the electron star in the next section since it is more settled and more literatures have been done toward this direction.

3.3 Electron star

In this fluid approximation, the claim is that the total charge of the system is made up by infinitely many electrons whose charge q is much smaller than the total charge $\langle Q \rangle$, $q \ll \langle \mathcal{Q} \rangle$. The gravity side is still restricted to be classical gravity limit i.e. $\kappa^2/L^2 \ll 1$. From the locality in r, we demand that the Compton wavelength of the bulk spinor ($\sim m^{-1}$) is much less than

[1] We can Fourier transform the bulk spinor field to get rid of the x^μ dependence. The Dirac equation will then becomes ODE's with only r dependence. This is similar to solving Schrődinger equation in a weird potential.

the *AdS* radius L i.e. $mL \gg 1$ [87]. The equations of motion of the gravity coupling to the fluid are [85]

$$\mathcal{R}_{AB} - \frac{1}{2}g_{AB}\mathcal{R} - \frac{3}{L^2}g_{AB} = \kappa^2\left(\frac{1}{q^2}\left(F_{AC}F_B^C - \frac{1}{4}g_{AB}F_{CD}F^{CD}\right) + T_{AB}\right) \tag{3.12}$$

and

$$\nabla_A F^{AB} = q^2 J^B \tag{3.13}$$

The energy-momentum tensor and the current can be expressed in the perfect fluid's variables, namely the four vector u^A, energy density ρ, the pressure p and the number density σ as

$$T_{AB} = (\rho + p)u_A u_B + p\, g_{AB}\ ; \qquad J_A = \sigma u_A\ ; \qquad -p = \rho - \mu_{\text{local}}\sigma \tag{3.14}$$

We can do the coordinates transformation to the centre of mass frame and set $u^A = (e_t^t, 0, 0, 0)$, where e_a^A is the inverse veilbein defined in the appendix A. The fluid variables can be realted to the spinor field by adding the Dirac action (A.1) to the Einstein-Maxwell action (2.29) then calculate T^{AB} and J^A as shown explicitly in [83]. Using this procedure, we find that

$$\rho = K\int_m^{\mu(z)} dE\ E^2\sqrt{E^2 - m^2}\ ; \qquad \sigma = K\int_m^{\mu(z)} dE\ E\sqrt{E^2 - m^2} \tag{3.15}$$

where K is a proportional constant of order N^0 and $\mu(z)$ is the μ_{local} defined in section 3.2.

A few more detail regarding how to obtain the equations of motion in terms of the fluid variables can be found in the Appendix C. For now I will just present the results from [85, 88]

$$ds^2 = L^2\left(-\frac{1}{r^{2z}}dt^2 + \frac{g_\infty}{r^2}dr^2 + \frac{1}{r^2}(dx^2 + dy^2)\right)\ ; \qquad A = \frac{h_\infty}{r^z}\frac{qL}{\kappa}dt \tag{3.16}$$

where the expressions for z, g_∞ and h_∞ in terms of the parameters in our theory is given in [85]. By varying parameters in the gravity side, one found that **the dynamical exponent** z diverges as $\hat{\beta} \equiv q^2L/\kappa \to 0$ and has an asymptotic value of order one when $\hat{\beta} \to \infty$. The large $\hat{\beta}$ region is more interesting to this section since the backreaction can be neglected for small $\hat{\beta}$ [85]. For a general z, this metric is called **Lifshitz spacetime** [89] illustrated in FIGURE 3.3. These weakly interacting fermions are contained within the radius $r > r_s$ and stabilised under the gravitational potential (see FIGURE 3.3 - RIGHT) in the same way as in the neutron star case [90]. Also, the fact that the electrons fluid parameters vanish at a definite radius $r = r_s$ means that it is not some kind of a gas that disperses all over the space. Therefore, we call it an "**electron star**".

However, the infinitely many electrons' modes in the bulk implies the field theory with infinitely many surfaces in the boundary. This feature is clearly unrealistic. Nevertheless, it could still be a good starting point to develop more realistic models since the bulk gravity theory is known. So let's see what are the other properties this electron star have.

We should also look at the thermal entropy and use the Luttinger count to check that the electron star does not have the same problem as the AdS RN. By fitting the numerical results,

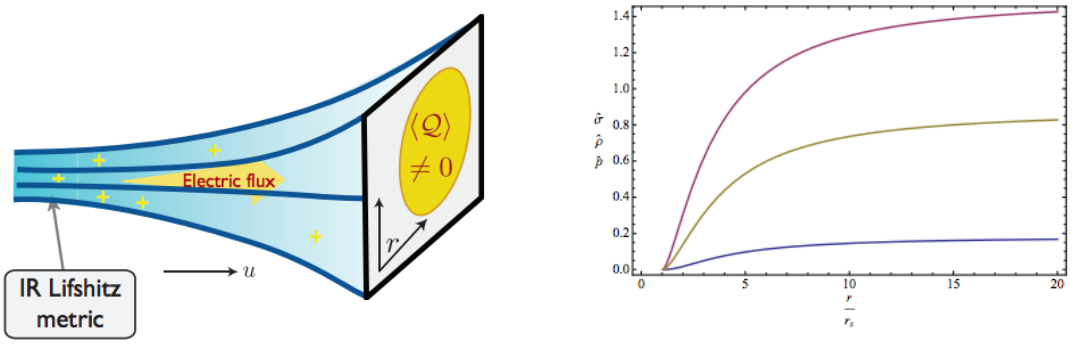

FIGURE 3.3: **LEFT**: The Lifshitz spacetime with the horizon at $r \to \infty$. All the electric flux in the bulk is sourced by the fermion gas hovering in the bulk. **RIGHT** From bottom to top, the pressure, energy and charge density distributions for an electron star. The position $r = r_s$, where all these fluid variables are all vanish, is interpreted as the "edge" of the star. These two figures are taken from [33] and [85] respectively

Ref [91] found that the entropy of such system is $\sim T^{2/z}$. The Luttinger count is also verified as there is no electric flux emanating from the horizon [87]. This means that the electron star is not degenerate and consists of fermions with the same symmetry as the Fermi liquid.

One can use the semiclassical analysis to see the behaviour of the decay rate of the electron star as in Ref [87]. This could be done by writing the equation of motion of the rescaled Dirac field $\chi = (|g|g^{rr})^{\frac{1}{4}}\,\Psi$, where Ψ is the original bulk spinor field in (A.1), in the form

$$-\frac{d^2\chi}{dr^2} + V(r)\chi \quad = \quad 0 \tag{3.17}$$

Here the Dirac equation for χ took the same form as the Schrődinger equation with the "energy" eigenvalue equals to zero. This allows us to use the semiclassical approximation such as the WKB method. The potential at different values of k looks like the diagrams below.

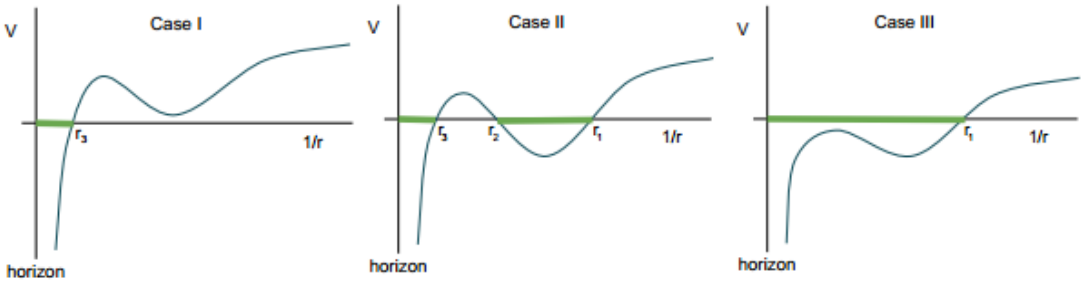

FIGURE 3.4: The potential $V(r)$ of the WKB Dirac equation as a function of $1/r$ with the Lifshitz horizon $r \to \infty$ located at the origin. The potentials in case I, II and III can be obtained by tuning the boundary momentum k^2. The thick green lines represent the location of the zero "energy" state in (3.17). Note that stable zero "energy" bound states can be found only in the $r_1 \leq r \leq r_2$ in case II This figure is taken from [87]

In the case I, there is no stable state at all. The zero energy state stuck in the region $r > r_3$ and will eventually fall behind the horizon [60]. In case II, there will be many almost stable zero energy state with an exponentially small amplitude of the tunnelling from $r_1 \geq r \geq r_2$ to the

horizon. The negative "energy" bound states can occur in case III but no boundary with zero "energy". As a result, the retarded Green function has poles only in the parameters ranges of case II. One can calculate the decay rate or the self-energy from the tunnelling rate and find that it is an exponential function. [21, 87]

$$\Sigma \quad \propto \quad \exp\left\{A\left(k_F^z/\omega\right)^{\frac{1}{z-1}} + B\right\} \tag{3.18}$$

where A and B are some constants that depend on parameters in our theory. This means that the decay rate of the excitation with low ω is exponentially small. Hence the quasi-particle excitations of the dual field theory are very long-lived, even longer then those of Landau-Fermi liquid.

To sum up, the electron star is the well-understood gravity model of the fermions. However, it does not represent any known metal due to the fact that it is dual to the field theory with too many Fermi surface and too stable excitation.

3.4 Adding the Dilaton

The Lifshitz geometry, as a result of the backreaction in the electron star case, can be mimicked when we include the dilaton into our gravity model. The action in the bulk then becomes the Einstein-Maxwell-Dilaton action (EMD) which has the following form [52, 81, 92]

$$S_{EMD} \quad = \quad \int d^{d+1}\sqrt{|g|}\left[\frac{1}{2\kappa^2}\left(\mathcal{R} - 2|\nabla\Phi|^2 - \frac{V(\Phi)}{L^2}\right) - \frac{Z(\Phi)}{4q^2}F_{AB}F^{AB}\right] \tag{3.19}$$

where $V(\Phi)$ and $Z(\Phi)$ are functions of Φ that we can choose later. According to [92], we may assume the exponential behaviour, $V(\Phi) = V_0 e^{2\beta\Phi}$ and $Z(\Phi) = e^{2\alpha\Phi}$, in the IR region. In general, the metric resulting from this action can be written as [52]

$$ds^2 \quad = \quad L^2 r^{2\delta}\left(-\frac{dt^2}{r^{2z}} + \frac{g_\infty}{r^2}dr^2 + \frac{1}{r^2}dx^i dx^i\right) \tag{3.20}$$

where α, β, δ are some constants.

In general, the dilaton Φ is not constant but grow logarithmically with r i.e. $\Phi \propto \log r$ [52, 92]. This leads us to be concerned about the higher derivative corrections required to stabilise the dialton at a constant value. However, in the presence of ideal fluid in the bulk (e.g. electron star), there exist the IR solution where the dilaton is a constant [60]. The theory is said to be a fixed point under the RG transformation $r \to \lambda r$ in the $r/L \gg 1$ region. In this case, we are back to the Lifshitz spacetime in (3.16) with $\delta = 1/2$ and the critical exponent z identified as

$$z = \frac{1}{1 - h_\infty^2 Z(\Phi)} \qquad \text{where} \qquad A = \frac{h_\infty}{r^z}\frac{qL}{\kappa}dt \tag{3.21}$$

The different metric can be obtained when we move away from this fix point as illustrated in FIGURE 3.6. This will be discussed in more detail in section 3.4.2.

There are number of works studied the EMD theory over the past few years (see [92, 93] for reviews and [94] especially for the fermion). However, I will only focus on two aspects of it namely

(i) The dilaton is used to produce a "hard wall" that terminates the metric at some finite $r = r_0$. This can be done by forcing the dilaton Φ to be in the form $\Phi \sim \ln(\Theta(r_0 - r))$, where $\Theta(x)$ is a step function.

(ii) As outlined earlier, the different phases in the deep interior $r \to \infty$ can be obtained by adding the relevant perturbation to the EMD action. This will be discussed in the more detail in section 3.4.2.

3.4.1 Hard wall : AdS_4 with confining geometry

The confining geometry of this type was first introduced in the study of hardronic/mesonic phase in AdS/QCD [95, 96]. Similar to the case of Hawking-Page transition we discussed in section 2.6, all gauge degree of freedoms in the dual field theory are confined.

Let's look at the some applications from the condensed matter side. In the holographic study of the superfluid-insulator phase transition, the confining geometry is introduce to put an energy gap that get rid of the low energy degree of freedom [97, 98]. In the context of the fermi liquid, fermions in the confining bulk metric should corresponds to the weakly interacting fermions in the boundary since they can no longer interact with each others via the massless gauge field. The fermions in dual field have exactly the same properties as a weakly interacting fermions in the Landau-Fermi liquid!

In this holographic model for Landau-Fermi liquid in 2+1dimensional boundary, the metric is just a standard AdS_4 that terminates at the **hard wall**, $r = r_0$ [99]. By doing the Fourier transform to get rid of the boundary spatial dependence, we can write down the Dirac equation as a 1d problem as

$$\left(i\sigma^2\frac{d}{dr} - \sigma^1\frac{m}{r} - k\sigma^3 - qA_t\right)\chi_{l,k}(r) \quad = \quad E_l(k)\chi_{l,k}(r) \tag{3.22}$$

where $\chi(z)$ is the normalisable mode of the bulk spinor field rescaled by factor $(|g|g^{rr})^{\frac{1}{4}}$. The hard wall at $r = r_0$ requires a boundary condition

$$\chi_1^\dagger(r_0)\sigma^2\chi_2(r_0) = 0\ ; \qquad \chi(z \to 0) \sim z^m \tag{3.23}$$

for any two Dirac spinors χ_1, χ_2. We can also normalise the spinor field by demanding that

$$\int_0^{r_0} dr\chi^\dagger(r)\chi(r) \quad = \quad 1 \tag{3.24}$$

First thing to notice is that, in the absence of the background gauge field, one can solve this eigenvalue equation exactly. There are many bulk solutions with many energy levels, similar to the solution of the Schrődinger equation of a particle in the 1d box. One can then turn on the

small flux A_t and increases the chemical potential so that it has a value between first and second energy level as shown in FIGURE 3.5. The solutions χ in the non-zero flux has to be solved self-consistently such that there is no flux passed through the hard wall. This procedure makes the hard wall model obeys the Luttinger count by construction. The more details numerical procedures can be found in [99]. We also notice that this set up has no event horizon which means it is at zero temperature and has zero thermal entropy.

This model is extremely powerful in a sense that it requires neither the fluid approximation, as for the electron star[85, 86, 91], nor fermion bilinear with a zero frequency contribution, as in the Dirac hair [83]. Moreover, it really gives only one Fermi surface with a well-understood gravity theory.

The fact that the structure of Landau-Fermi liquid theory is captured in a quite simple gravity theory is indeed astonishing. However, the duality between the hard wall bulk and the Landau-Fermi liquid is a weak to weak duality. If our aim is to study the strongly correlated electron system, we need to modify this gravity in to something that gives the strongly interacting boundary theory. There are number of developments from this model toward this direction. The behaviour of the hard wall Fermi liquid state when the hard wall is taken away has been studied in the model called "**quantum electron star**" [100]. The alternative confining metrics called **the AdS soliton** have been applied in [101, 102]. The behaviour of this hardwall model and the quantum electron star under a strong magnetic field has also been studied in [103] and found the lowest Landau level as well as in the quantum hall experiment.

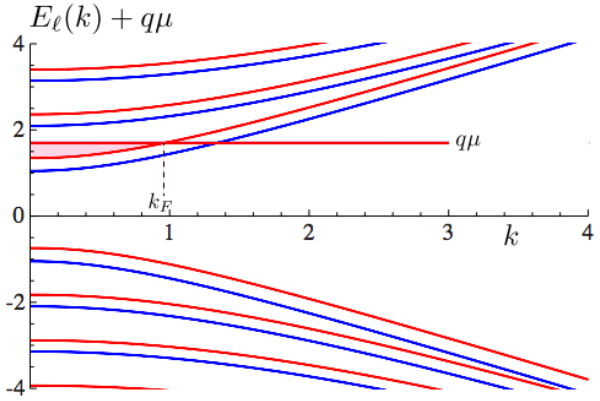

FIGURE 3.5: The dispersion relation obtained from the fermion hard wall model [99]. The blue line is the dispersion relation $E_l(k)$ when $A_t = 0$. The value of $E_l(k)$ received a small correction when $A_t(r = 0) = \mu$ is turned on. We can now see an intersection between $E_l(k)$ and $q\mu$ at $k = k_F$. This is indeed the momentum k_F of the one and only Fermi surface.

3.4.2 Fractionalised phase and hidden fermi surface

In this section, we consider the gravity theory with the dilaton and the charge fluid. The fluid's parameter's namely, the energy density E and the charge density Q are fixed. The metric

of this system at the zero temperature can be written as

$$ds^2 = L^2\left(-f(r)dt^2 + g(r)dr^2 + \frac{dx^2+dy^2}{r^2}\right) \;; \qquad A = \frac{eL}{\kappa}h(r)dt \tag{3.25}$$

For the computational simplicity, one can set $Z(\Phi) \approx 1$ and $V(\Phi) \approx -6 - 4\Phi^2$. The near boundary expansion takes the form

$$\begin{aligned} f(r) &= \frac{1}{r^2} + \ldots \qquad ; \qquad g(r) = \frac{1}{r^2} + \ldots \\ h(r) &= \frac{\kappa}{eL}\left(\mu - Qr + \ldots\right) \qquad ; \qquad \Phi(r) = \phi_0 r + \frac{\langle O\rangle}{2}r^2 + \ldots \end{aligned} \tag{3.26}$$

where ϕ_0 and $\langle O\rangle$ are the expectation values of the dilaton and the operator O dual to the bulk dilaton Φ [60]. Thus, the theory near the bounder is characterised by the sources $\{\phi_0, \hat{\mu}\}$ and the responses $\{E, Q, \langle O\rangle\}$. The parameter $\hat{\mu}$ is the reduced chemical potential μ expressed in the unit of eL/κ.

In the IR region, there are three possible scenarios depending on the ratio of $\phi_0/\hat{\mu}$. At a certain "critical" value of ϕ and $\hat{\mu}$, the boundary theory undergoes the RG flow toward the Lifshitz fixed point as mentioned at the beginning of section 3.4.

$$\begin{aligned} f(r) &= 1/r^{2z} \qquad ; \qquad g(r) = g_L/r^2 \\ h(r) &= h_L/r^{2z} \qquad ; \qquad \Phi(r) = \phi_L \end{aligned} \tag{3.27}$$

In this metric, the temperature can be introduced by introducing the black brane. The metric in the presence of the black brane is found to be [81]

$$f_T(r) = f(r)\left(1 - (r/r_0)^{3(1+z)}\right) \;; \qquad g_T(r) = g(r)\left(1 - (r/r_0)^{3(1+z)}\right)^{-1} \tag{3.28}$$

One can calculate the area of the horizon and see that the entropy $S \propto T^{1/z}$. This implies that the zero temperature state is not degenerate. Next, we can also use the Luttinger count to check whether the total electric field in the bulk is sourced by the fluid or not. The mismatch in the Luttinger count can be expressed in term of the electric flux that pass through the horizon i.e. $\int_{\mathbb{R}^2} \star[Z(\Phi)F]$. At zero temperature, the horizon of this Lifshitz geometry is at $r_0 \to \infty$ as in the AdS_4 case. The flux in this case behaves like r_0^{-2}. Hence, there is no flux emanating from the Lifshitz horizon and the total electric field is sourced by just the fluid. In [77], this phase is called **cohesive phase**

To get away from this Lifshitz fix point, we perturb the Lifshitz fix point by a relevant operator. The perturbed IR metric looks like

$$\begin{aligned} f(r) &= 1/r^{2z}\left(1 + \delta f r^M\right) \qquad ; \qquad g(r) = g_L/r^2\left(1 + \delta g r^M\right) \\ h(r) &= h_L/r^{2z}\left(1 + \delta h r^M\right) \qquad ; \qquad \Phi(r) = \phi_L\left(1 + \delta\phi r^M\right) \end{aligned} \tag{3.29}$$

with the scaling exponent $M > 0$. The boundary theory that has the ratio $\phi_0/\hat{\mu}$ different from the value of the Lifshitz fixed point will be hit by this relevant deformation and flows away from

the fixed point as illustrated in FIGURE 3.6. There are two extreme IR geometries characterised by two dilaton profiles [60] namely

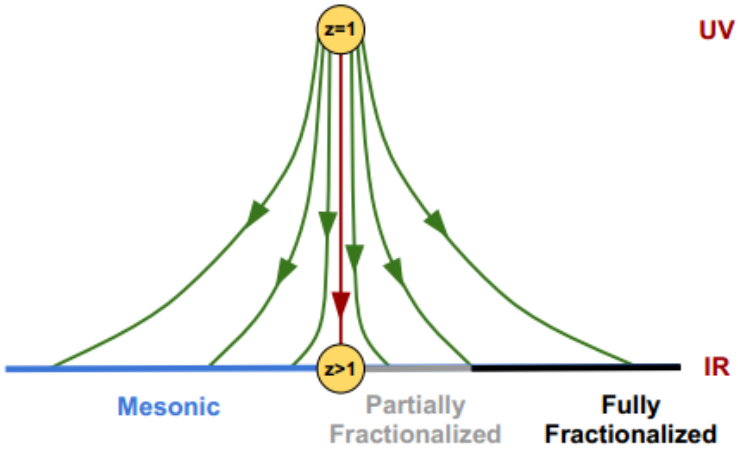

FIGURE 3.6: The three possible IR geometries as a result of the RG flow from the UV AdS_4 metric. The fractionalised, partially fractionalised and cohesive(mesonic) phase is shown from the right to left respectively. The term "mesonic" has been used in [60] where this picture is taken from. However, it was realised in [77] that the name "mesonic" is misleading. Hence, I will use the term cohesive phase for the "mesonic" phase in this figure.

$\Phi \to \infty$ **:** The effective Maxwell coupling $q/\sqrt{Z(\Phi)}$ is negligible. The local chemical potential defined in 3.11 becomes $\mu_{\text{local}} \sim r^{-1} \to 0$. It follows that there will be no fluid in the large r region. In contrast, the electric flux from the Lifshitz horizon, $\int_{\mathbb{R}^2} \star[Z(\Phi)F]|_{r\to\infty} \sim$ const, indicates that there is a nonzero electric flux emanating from the horizon. For a reason that will becomes clear later, this phase is called **the fractionalised phase**.

$\Phi \to -\infty$ **:** In this case, the effective Maxwell coupling becomes large. The local chemical potential is constant at $r \to \infty$. The vanishing electric flux at large r, $\int_{\mathbb{R}^2} \star[Z(\Phi)F]|_{r\to\infty} \sim r^{-7/3} \to 0$, means all the electric field is generated from the fluid matter in the bulk. This theory of gravity is therefore describing the cohesive phase as in the Lifshitz geometry.

A careful Luttinger count in [60] found that in the regime $\Phi \to \infty$ there is a range of $\phi_0/\hat{\mu}$ for which the electric field is sourced by both bulk fluid and the Lifshitz horizon. This phase is labelled as the partially fractionalised phase shown in FIGURE 3.6. We now see that the EMD action can capture various zero temperature phases of the boundary field theory, similar to the phase transitions in the cuprate shown in FIGURE 1.5.

Now, let's see why the phase with the non-zero flux emitted from the horizon is called the fractionalised phase. The name **"fractionalisation"** came from quantum phase transition literatures where we can treat an elementary particle (e.g. electrons) as a composite particle. For example, the electron can be thought of as a spin and charge particle glued together by some **emergent gauge field** [22].

Let's look at an example that is relevant to our discussion in FIGURE 3.7. Consider the mixture between electrons that are stuck on the lattice sites and the free electrons, called the **Kondo lattice**. The magnetic moment is formed by the electron in the f-orbital [16] and hence

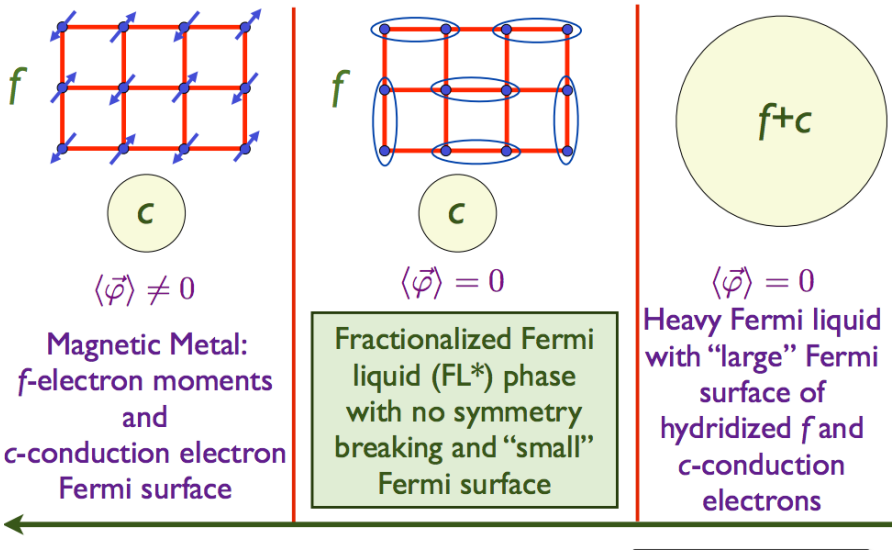

FIGURE 3.7: The zero temperature phase diagram of Kondo lattice. **LEFT :** The phase with c-electron Fermi surface and antiferromagnetic order $\varphi \neq 0$ that breaks U(1) symmetry. **RIGHT :** The f-electrons are no longer localised on the lattice. Both f and c electrons form a Fermi surface. **MIDDLE :** An intermediate phase between LEFT and RIGHT. The f-electrons deconfine into z-fermion and spin degree of freedom. The z-fermions also form a Fermi surface but it was "hidden" and hence not shown in the above figure. This figure is taken from [104]

we call these localised electrons **f-electrons**. The free electrons are said to be in the conducting band and hence called **c-electrons**. The creation operator of the electron that are stuck at the lattice site i can be written as

$$f_{i,\alpha} = e^{-i\vartheta_i} z_{i,\alpha} \qquad \text{where} \qquad e^{-i\vartheta_i} \equiv b_i \tag{3.30}$$

We define $f_{i,\alpha}, z_{i,\alpha}$ to be spinor operators and b_i to be the bosonic operator describing the direction of the spin through the angle ϑ_i. This decomposition implies that there is another **"emergent"** local U(1) transformation other than $f_{i,\alpha} \to e^{i\theta_i} f_{i,\alpha}$, namely

$$b_i \to e^{i\phi_i} b_i \; ; \qquad z_{i,\alpha} \to e^{-i\phi_i} z_{i,\alpha} \; ; \qquad f_{i,\alpha} \to f_{i,\alpha} \tag{3.31}$$

One can associate this emergent U(1) local symmetry with the emergent U(1) gauge field that glue b_i and $f_{i,\alpha}$ together. The interesting part of FIGURE 3.7 is the middle part, where the parameters are tuned such that the field $f_{i,\alpha}$ and b_i are deconfined and behave as two separate entities [105]. The spinor $z_{i,\alpha}$ form a Fermi surface as well as the c-electrons. The difference here is that the Fermi surface of the z fermions is charged under an emergent U(1) gauge field.

The Fermi surface of the c-fermions can be observed by reading off the pole of the Green function of a probe particle. However, this type of probe can only detect the gauge invariant operator. This type of probe cannot detect the Fermi surface of the z-electron and that causes the mismatch in the Luttinger count. Thus, the Fermi surface of the z-electrons is said to be **hidden** [79]. This phase with deconfined f-electrons is the non-Fermi liquid, since the Luttinger count is violated, and is usually called **fractionalised fermi liquid** (FL*)[106]

We can see that the FL* phase in FIGURE 3.7and the partially fractionalised phase in FIGURE 3.6 are remarkably similar. Both phases have two Fermi surfaces, one is detectable by a probe fermion and the other is hidden. Hence, we can associate the charge behind the horizon in EMD theory with the "hidden" z-fermion in the Kondo lattice.

Although the EMD theory does not have all exactly the same properties as the Kondo lattice model, it gives us a hint of that we may interprete the charge matters behind the horizon as hidden Fermi surfaces. Moreover, the further holographic studies [81] found the way to detect the hidden Fermi surface using the entanglement entropy. The entanglement entropy, that we discussed in section 1.3.4 and 2.6, for the system with hidden Fermi surface is found to be

$$S_E \quad \propto \quad \mathcal{Q}_{\rm hid}^{2/3}{\rm Vol}(\Sigma)\ \ln\left(\mathcal{Q}_{\rm hid}^{2/3}{\rm Vol}(\Sigma)\right) \tag{3.32}$$

for the 2+1d field theory [81]. Here, $Q_{\rm hid}$ is the flux sourced by the hidden fermions and Vol(Σ) defined in section 2.6 is the perimeter of the region B in FIGURE 2.9. The non-zero S_E for $\mathcal{Q}_{\rm hid} \neq 0$ indicates that the quantum entanglement has some roles behind the existence of the FL* phase. The entanglement here is also long ranged since it depends on Vol(Σ) ln Vol(Σ) instead of Vol(Σ) alone.

3.5 Closing

Concluding the literature review of the topics that is developing at the rapid speed is probably as difficult as writing the history of a war when it is still raging. I cannot end it by suggesting all interesting work that could been done in a past few years. However, I can say something about the interesting topics that I capable of learning and summarising over the past few months. That is the following.

So far in this review, I discuss about basics AdS/CFT correspondence developed over a decade ago up to the recent work on hidden Fermi surface in early 2012. In the first chapter the heuristic arguments that, hopefully, will convince people that the $\mathcal{N}$=4 super Yang-Mills theory is dual to the semiclassical theory of gravity in $AdS_5 \times S^5$. Then, the brief introduction to the theory of fermions and quantum phase transitions are presented. The point of this introduction is to explain why the quantum many-body problem is hard and interesting due to its quantum nature. It turns out that the holographic duality might be able to give us some insight about these many-body problem, as mentioned in the text. The holographic dictionary rules for building the bottom-up gravity model and extracting physical quantities are discussed in chapter 2. Finally, in chapter 3, one finds a superficially introduction of the popular bottom-up models of fermions such as AdS Reissner-Nordstrőm, electron star, hard-wall and the Einstein-Maxwell-Dilaton theory. In the appendices, I put the detailed calculation one can use to extract correlation function from the gravity theory and the mathematica code that I use to play with Einstein-Maxwell equations.

There are many other works along the direction of holographic (non-)Fermi liquid that I cannot put in this dissertation. The quest for the understanding of the fermions system,

especially the cuprate which is the main theme of this dissertation, is still on going. There gravity dual of the different phases in the cuprate phase diagram proposed but the model that unifies all these phases are still missing. There are models built to study the pairing mechanism of the electrons using the the mixture between the electrons and bosons [107, 108]. The quantum correction and the lattice, which should improve the accuracy of the AdS/CFT prediction, have also been studied [70, 71, 100, 101]. I would also like to emphasis on the quantum information aspects that are open up by the holographic realisation of the entanglement entropy. The recent applications of the holographic principle to the non-equilibrium system would also be interesting since we can use entanglement entropy to study the evolution of the quantum state, see e.g. [109]. The Ryu-Takayanagi formula can be very powerful in the studies of such non-equilibrium quantum system since it allows us to study the entanglement structure in higher dimensions systems. The other most interesting arena for quantum information and condensed matter is the gapped topological state such as quantum hall[2] and topological insulator, which are one of the candidates for quantum computation. As a result, there have a lot of quantum information studies in these systems, see e.g. [110–112]. The recent holographic studies found the systems that resemble the quantum hall state namely the model of intersecting branes [113–115] and the electron star under the strong magnetic field [103]. These models open up the possibility that there are theories of gravity dual to the candidates for quantum computer! It would be really interesting to see either the physics of the black hole helps building the quantum computer or the quantum simulator that can be used to study the black hole.

From the non-string perspective, there are a whole quantum world out there, which is largely unexplored. This is because it is only now or in a last decades or so, that we are developing the technological capability to scale up quantum system, to manipulate them, to test them in the lab and try compare the data with the theory. Surely, this is the time when a lot of new theories and ideas are flourishing. People are not exactly sure what are these quantum theories, including AdS/CFT, going to be developed in to and I think that makes it so exciting.

[2]The quantum hall state can be realised by putting the 2d electrons under the strong magnetic field background to the low temperature [110]

Appendix A

Solving Dirac equation

I fill up some steps in the solving the Dirac equation outlined in [21, 62]. The correlation function is calculated using the formalism in [53]. I will focus on the AdS_4 and $AdS_2 \times \mathbb{R}^2$ spacetime for simplicity. The calculations presented here are collected from various papers namely [53, 54, 62, 67, 68, 94].

A.1 Setup

Firstly, the spinor has more than one complex component, unlike the scalar. It is known that, for any dimension, the dimension of the boundary fermionic operator is always half of that of the bulk field[62]. The real-time action of the Dirac equation in the bulk is

$$S_{\text{Dirac}} = -\int d^{3+1}x\sqrt{|g|}(\bar{\Psi}\Gamma^A\mathcal{D}_A\Psi - m\bar{\Psi}\Psi) + S_{\text{bnd}} \tag{A.1}$$

where S_{bnd} is the term we need to add to make the variational principle well-defined and have the appropriate boundary condition. Here, I denote Ψ for the bulk spinor and ψ for the spinor operator in the boundary. The Dirac equation obtained from this action is

We need to be careful about the Γ^A and $\mathcal{D}_A$. Γ^A is not the standard Gamma matrices in the flat space that we used in QFT course. We can related these matrices to the one we know by the veilbein formalism. The idea of this formalism is simply write down the metric as [12]

$$g_{MN}(x) \quad = \quad \eta_{ab}e^a_M(x)\, e^b_N(x) \tag{A.2}$$

where η_{ab} is the flat spacetime metric. The object $e^M_a(x)$ is called the **veilbein**. Sometimes, like in [53, 54], the veilbein indices a, b is called the tangent spacetime indices. The objects in the curved spacetime, e.g. the Gamma matrices, can be expressed in terms of the flat spacetime expressions through the inverse veilbein.

$$\Gamma^M \quad = \quad \Gamma^a e^M_a; \qquad \{\Gamma^a, \Gamma^b\} = 2\eta^{ab}\mathbb{1} \tag{A.3}$$

The covariant derivative is also not as simple as in the scalar. For the vector in curve space, we have to add the Christoffel symbols to the derivative to act as the connection. Similar procedure is required for the spinor, but instead of the Christoffel symbols, one needs to add the spin connection term i.e.

$$D_M = \partial_M + \frac{1}{4}\omega_{M,ab}\Gamma^{ab} - iqA_M \tag{A.4}$$

where

$$\Gamma^{ab} = \frac{i}{2}[\Gamma^a, \Gamma^b]\,; \qquad de^a = \omega^{ab}e^b$$

For now, let's assume that we have the S_{bnd} which gives the Dirac equation and see how we can solve it. The Dirac equation in curved space has the following form

$$\left(e_a^M\Gamma^a\left(\partial_M + \frac{1}{4}\omega_{M,ab}\Gamma^{ab} - qA_\mu\right) - m\right)\Psi = 0 \tag{A.5}$$

The spin connection can be removed by redefine [2]

$$\Psi = (|g|g^{rr})^{\frac{1}{4}}\begin{pmatrix}\chi_+\\ \chi_-\end{pmatrix} \tag{A.6}$$

where $\chi_\pm$ is the eigenvector of Γ^r with eigenvalues ± 1. The Dirac equation is reduced into

$$\sqrt{\frac{g_{xx}}{g_{rr}}}\Big(i\sigma^2\partial_r - \sqrt{g_{rr}}\sigma^1 m\Big)\chi_\pm(r,k^\mu) = -\Big(\pm k - \sqrt{\frac{-g_{xx}}{g_{tt}}}(\omega + qA_t)\Big)\chi_\pm \tag{A.7}$$

where we use the rotational symmetry of the boundary theory to choose $k^\mu = (\omega, k, 0, 0)$. The choice of Γ^M here follows from [2, 62] namely

$$\Gamma^{\bar{r}} = -\sigma^3 \otimes \mathbb{1}\,; \qquad \Gamma^{\bar{t}} = i\sigma^1 \otimes \mathbb{1}\,; \qquad \Gamma^x = -\sigma^2 \otimes \sigma^1 \tag{A.8}$$

A.2 The Solutions and Correlation Functions

For the spacetime with an asymptotic AdS boundary, the solution near the boundary is found to be [53]

$$\begin{pmatrix}\chi_+\\ \chi_-\end{pmatrix} = \begin{pmatrix}A(k)r^{-mL}\\ D(k)r^{mL}\end{pmatrix} + \begin{pmatrix}B(k)r^{mL+1}\\ C(k)r^{-mL+1}\end{pmatrix} + \dots \tag{A.9}$$

where A, B, C, D are 2-component vectors which are related to each others i.e. $A \propto C$, $B \propto D$. We might think that we can fix the first term (A, D) as a source and treat (B, C) as a response. However, we cannot do that since B, C depend on A, D. Moreover, the boundary operator ψ has only 2 components while Ψ has 4 components. This indicates that we can fix only one of A or D to be a source.

In order to find out whether A and D are normalisable or non-normalisable, we have to see if the energy for a given mode is finite or infinite. It turns out that the energy of this asymptotic

solution takes the from [54]

$$\mathcal{E} \sim \int dr \, \frac{1}{r^4}\left[\bar{C}Ar^{4-2mL} - \bar{B}Dr^{4+2mL}\right] \tag{A.10}$$

From this, we can see that [53, 54]

(i) $mL \geq 1/2$: The term $\bar{B}D$ is normalisable while $\bar{C}A$ is non-normalisable. Hence, we should fix A as a source i.e. $\chi_+ = 0$ at the boundary.

(ii) $mL \leq 1/2$: The story is inverses and we have to fix $\chi_- = 0$ at the boundary instead.

(iii) $-1/2 < mL < 1/2$: both term are normalisable and we have a choice to choose either χ_+ or χ_- to be a source.

The two different boundary conditions in (i) and (ii) result in two different conformal field theories. They are often referred to as standard and alternative quantisation respectively. The scaling dimension of the conformal operator O_ψ of the former case is $\Delta^{(i)} = 3/2 + mL$ while the latter is $\Delta^{(ii)} = 3/2 - mL$. An intensive work on the case (iii) can be found in [54].

I will follow [53] and focus on the case (i). The Dirichlet boundary condition, $\delta S_{\text{bnd}} = 0$ implies that the real-time canonical momentum conjugate to the source $\Psi_+ \equiv +\Gamma^r\Psi_+$ are

$$\Pi_+ = -\sqrt{|g|g^{rr}}\bar{\Psi}_- \tag{A.11}$$

By setting $\chi_+ = 0$, the 1-point function can be found using the formalism outlined in section 2.3.1.

$$\langle \bar{O}_\psi \rangle = \lim_{r\to 0} r^{3/2-m}\Pi_+ \qquad \text{i.e.} \qquad \langle \bar{O}_\psi \rangle = \bar{D} \tag{A.12}$$

and the retarded Green function $G_R(t,\mathbf{x}) = i\Theta(t)\langle[O(t,\mathbf{x}), O^\dagger(0,\mathbf{0})]\rangle$ is

$$G_R(\omega,\mathbf{k}) = DA^{-1} = i\mathcal{S}(\omega,\mathbf{k})\Gamma^t \tag{A.13}$$

where $AA^{-1} = i\Gamma^t$ and $\mathcal{S}(k)$ is a matrix that satisfies $D = \mathcal{S}(k)A$ [53]

A.3 Fixing S_{bnd} term

With out S_{bnd} term in (A.1), once we varying $\Psi \to \Psi + \delta\Psi$, the change in action will be

$$\begin{aligned}\delta S_{\text{Dirac}} &= \text{bulk terms} - \delta\int d^{3+1}x\sqrt{|g|g^{rr}}(\bar{\Psi}_-\partial_r\Psi_+ - \bar{\Psi}_+\partial_r\Psi_-) \\ &\supset \int d^{2+1}x\sqrt{|g|g^{rr}}(\bar{\Psi}_-\delta\Psi_+ - \bar{\Psi}_+\delta\Psi_-)\end{aligned}$$

Thus, this means the action depends on both Ψ_- and Ψ_+. However,this is wrong as we cannot freely choose $\delta\Psi_+$ or Ψ_-, at least in case (i) and (ii). In case (i), Ψ_- becomes the response to the source Ψ_+ and δS_{Dirac} should not depend on $\delta\Psi_-$. We can fix this Ψ_- dependence by adding

an extra boundary term namely

$$S_{\text{bnd}} = -\int_{r=\epsilon} d^{2+1}x\,\sqrt{|g|g^{rr}}\bar{\Psi}_+\Psi_- \tag{A.14}$$

With this boundary term, the on-shell Dirac action becomes

$$\delta S_{\text{Dirac}} = -\int_{r=\epsilon} d^{2+1}x\,\sqrt{|g|g^{rr}}\big(\bar{\Psi}_-\delta\Psi_+ + \delta\bar{\Psi}+\Psi_-\big) \tag{A.15}$$

Now, δS_{Dirac} no longer has $\delta\Psi_-$ dependence hence this boundary term fix the earlier conundrum.

A.4 $AdS_2 \times \mathbb{R}^2$ Correlation Function

In the $AdS_2 \times \mathbb{R}^2$, the Dirac action can be written as

$$\big(e_a^A\Gamma^a\mathcal{D}_A - m + i\tilde{m}\,\Gamma\big)\,\Psi = 0 \tag{A.16}$$

where the metric background and the gauge field background is

$$ds^2 = \frac{R^2}{\zeta^2}(-dt^2 + d\zeta^2)\,; \qquad A_t = \frac{e_d}{\zeta} \tag{A.17}$$

where e_d is defined in (2.37). We have the only non-zero spin connection $\omega_{\bar{t},t\zeta} = \frac{1}{\zeta}$ from the veilbein $e^{\bar{t}} = (R/\zeta)dt$ and $e^{\bar{\zeta}} = (R/\zeta)d\zeta$. Here, I define $\bar{t}$ and $\bar{\zeta}$ to be the first and second component of the tangent spacetime respectively.

For the gamma matrices, I use

$$\Gamma^{\bar{t}} = i\sigma^1; \quad \Gamma^{\bar{\zeta}} = \sigma^3; \quad \Gamma = -\sigma^2 \tag{A.18}$$

where the term $\tilde{m}\Gamma$ came from the momentum in the $\mathbb{R}^2$ part of $AdS_2 \times \mathbb{R}^2$. This choice of gamma matrices is compatible with the choice I made in (A.8). The Dirac equation become

$$0 = \left[\frac{\zeta}{R}\big(\sigma^1(\omega + qA_t) + \sigma^3(\frac{1}{2\zeta} + \partial_\zeta)\big) - m - i\tilde{m}\sigma^2\right]\Psi \tag{A.19}$$

We can simplify this equation a little bit by rescale $\Psi = (|g|g^{\zeta\zeta})^{1/4}\chi = \Big(\sqrt{R/\zeta}\Big)\chi$ multiply the equation with σ^1

$$0 = \partial_\zeta\chi + \left[i\sigma^2(\omega + qA_t) - \frac{R}{\zeta}(m\sigma^3 + \tilde{m}\sigma^1)\right]\chi \tag{A.20}$$

Near the black brane boundary $\zeta \to 0$, we have

$$\zeta\partial_\zeta\chi = U\chi\,; \qquad U \equiv \begin{pmatrix} mR & \tilde{m}R - qe_d \\ \tilde{m}R + qe_d & -mR \end{pmatrix} \tag{A.21}$$

The solution of this equation has the following form

$$\chi \quad = \quad av_{-}\zeta^{-\nu} + bv_{+}\zeta^{\nu} \tag{A.22}$$

where a, b are some functions of ν and $v_{\pm}$ are the eigenvector of U with eigenvalues $\pm\nu$ respectively. This eigenvalue ν can be found by taking $\det[U - \nu\mathbb{1}] = 0$. We find that

$$\nu \quad = \quad \pm\sqrt{(\tilde{m}^2 + m^2)R^2 - q^2 e_d^2} \tag{A.23}$$

If we reexpress $\tilde{m}$ in terms of $\mathbb{R}^2$ momentum k, we will obtain ν_k in (3.6). Moreover, one finds very quickly that av_{-} is a non-normalisable mode and therefor the retard Green function is

$$\mathcal{G} \quad = \quad \frac{b}{a} \tag{A.24}$$

Recall that χ is invariant under $\zeta \to \lambda\zeta$, we can figure out the ω dependence in a and b namely

$$a \sim \omega^{-\nu}\,; \qquad b \sim \omega^{\nu} \tag{A.25}$$

and hence

$$\mathcal{G} \quad = \quad c(\nu)\omega^{2\nu} \tag{A.26}$$

as claimed in equation (3.5) in section 3.1

Appendix B

AdS Schwarzschild and The Black BraneTemperature

B.1 The AdS Schwarzschild Solution

In order to obtain the AdS metric, one need to look at the Einstein-Hilbert action with a negative gravitational constant. The action for that gives the asymptotic AdS_4 looks like

$$S = \int d^4x\sqrt{|g|}\left[\frac{1}{2\kappa^2}\left(\mathcal{R}+\frac{6}{L^2}\right)\right] \tag{B.1}$$

By varying the action, regardless the necessary boundary term, one should obtain the Einstein field equation

$$\mathcal{R}_{MN}-\frac{1}{2}g_{MN}\mathcal{R}-\frac{3}{L^2}g_{MN}=0 \tag{B.2}$$

The solution of this equation is assumed to be

$$ds^2=\frac{L^2}{r^2}\left(-f(r)dt^2+f(r)^{-1}dr^2+dx^idx^i\right) \tag{B.3}$$

where $f(r)$ is an unknown function that can be determined after we solve the Einstein field equation. Now, there are two ways one can see what $f(r)$ can be, namely

- Use the veilbein method introduced in the Appendix A. The vielbein of this metric can be listed as following

$$e^{\bar{t}}=\frac{L\sqrt{f}}{r}dt\ ;\qquad e^{\bar{r}}=\frac{L}{r\sqrt{f}}dr\ ;\qquad e^{\bar{i}}=\frac{L}{r}dx^i \tag{B.4}$$

  There are not many non-zero spin connections, namely

$$\omega^{\bar{t}\bar{r}}=\left(\frac{\sqrt{f}}{L}-\frac{r}{L}\frac{f'}{\sqrt{f}}\right)\ ;\qquad \omega^{\bar{i}\bar{r}}=\frac{\sqrt{f}}{L} \tag{B.5}$$

where $f' \equiv \frac{d}{dr} f$ and the vielbein index $\bar{i} = \{x, y\}$. The reason we need these vielbein and spin connections is that, the Ricci tensor in the tangent space basis can be written as

$$\mathcal{R}^{ab} = d\omega^{ab} + \omega^{ac}\omega^{cb} = \mathcal{R}^{ab}_{MN} dx^M \wedge dx^N \tag{B.6}$$

and we can turn $\mathcal{R}^{ab}$ back to $\mathcal{R}_{MN}$ using the inverse vielbeins e^M_a [7, 12]. This method might sounds complicated but I found that it is better than plug in the metric, calculating Christoffel symbols and then calculating the Riemann tensor.

- Find a good mathematica package that can find the Ricci tensor and Ricci scalar. I found the mathematica package call `diffgeo.m` extremely useful. One can find this package and the manual from Matthew Headrick's (the one who wrote this package) personal webpage http://people.brandeis.edu/~headrick/Mathematica/. The essential command line and the simplified expression on the LHS of (B.2) are

```
In[7]:= display[eqnR1 = Simplify[RicciTensor - metric RicciScalar / 2 - 3 metric ]]
```

Out[7]=

{r, r}	$-\frac{3-3\,f[r]+r\,f'[r]}{r^2\,f[r]}$
{t, t}	$\frac{f[r]\,(3-3\,f[r]+r\,f'[r])}{r^2}$
{x, x} {y, y}	$\frac{-6+6\,f[r]-4\,r\,f'[r]+r^2\,f''[r]}{2\,r^2}$

FIGURE B.1: The table displaying non-zero {M,N} components of the LHS of (B.2).

Using either methods, one should find that the equation that $f(r)$ has to satisfies is

$$0 \quad = \quad 3 - 3f(r) + r\frac{d}{dr} f(r) \tag{B.7}$$

For an asymptotic AdS_{d+1} spacetime, we can simply change 3 to d. With $f(r) = 1$, we obtain the AdS_4 metric but we also see that there is a solution of the form

$$f(r) \quad = \quad 1 - \left(\frac{r}{r_0}\right)^d \tag{B.8}$$

for any $0 < r_0 \leq \infty$. This is the AdS Schwarzschild solution that describes the black brane.

B.2 Black Brane Temperature

The method that used to extract the black hole temperature here is the Gibbons-Hawking trick [2]. Let's start by writing the metric in (B.3) in the Euclidean signature as

$$ds^2 \quad = \quad g_{\tau\tau}(r) d\tau^2 + \frac{dr^2}{g}^{rr}(r) + g_{ii}(r) dx^i dx^i \tag{B.9}$$

The black brane is located at $r = r_0$ where $g_{\tau\tau}(r_0) = g^{rr}(r_0) = 0$. Hence, we can expand the metric component at $r \to r_0$ as following

$$g_{\tau\tau}(r) = g'_{\tau\tau}(r_0)(r_0 - r) + \dots \; ; \qquad g^{rr}(r) = g'^{rr}(r_0)(r_0 - r) + \dots \tag{B.10}$$

where $g'_{\tau\tau}, g'^{rr}$ are the derivatives of $g_{\tau\tau}, g^{rr}$ Then, substitute the re-parametrisation $R = 2\sqrt{r_0 - r}/\sqrt{g'^{rr}}$. We will see that the AdS Schwarzschild metric has the form

$$ds^2 \quad = \quad dR^2 + \frac{1}{4}R^2 g'_{\tau\tau}(r_0) g'^{rr}(r_0) d\tau^2 \tag{B.11}$$

which is similar to the metric of the cylinder, $ds^2 = dR^2 + R^2 d\theta^2$. We know that both θ and τ are periodic variables under the transformation $\theta \to \theta + 2\pi$ and $\tau \to \tau + \beta$. Hence, once we demand that $d\theta = \frac{1}{2}\sqrt{g'_{\tau\tau}(r_0) g'^{rr}(r_0)}d\tau$, the periodic β is found to be

$$\beta = \frac{4\pi}{\sqrt{g'_{\tau\tau}(r_0) g'^{rr}(r_0)}} \tag{B.12}$$

Once we substitute the AdS Schwarzschild metric, $g'_{\tau\tau}(r_0) = L^2 f'(r_0)/r_0^2$ and $g'^{rr} = r_0^2 f'(r_0)/L^2$, the inverse temperature β becomes

$$\beta = \frac{4\pi}{f'(r_0)} = \frac{4\pi r_0}{d} \tag{B.13}$$

Appendix C

Playing with the Einstein-Maxwell equation of the electron star

The aim of this appendix is to clarify how one can solve the equations of motion, (3.12) and (3.13), in the electron star setup. The equations of motion and the fluid variables are redefined such that the constants q, κ are absorbed.

$$\mathcal{R}_{AB} - \frac{1}{2}g_{AB}\mathcal{R} - \frac{3}{L^2}g_{AB} = \left(F_{AC}F_B^C - \frac{1}{4}g_{AB}F_{CD}F^{CD}\right) + T_{AB} \tag{C.1}$$

and

$$\nabla_A F^{AB} = J^B \tag{C.2}$$

This procedure has been used in the original electron star paper [85]. The fluid variables $\{\rho, p, \sigma\}$ are re-parametrised to the new ones $\{\hat{\rho}, \hat{p}, \hat{\sigma}\}$ as following

$$\rho = \frac{1}{L^2\kappa^2}\hat{\rho}\,; \qquad p = \frac{1}{L^2\kappa^2}\hat{p}\,; \qquad \sigma = \frac{1}{qL^2\kappa}\hat{\sigma} \tag{C.3}$$

In order to solve the backreacted metric resulting from the presence of the electrons in fluid limit, the background metric and 1-form gauge field are assumed to have the form

$$ds^2 = L^2\left(-f(r)dt^2 + g(r)dr^2 + \frac{dx^2+dy^2}{r^2}\right)\,; \qquad A = \frac{qL}{\kappa}h(r)dt \tag{C.4}$$

It is not easy to find an equation of motions of these variables $f(r), g(r), h(r)$ in terms of the fluid variables that was presented in [85]. The rest of this section are essential pieces of the mathematica code I used to derive the equations of motion.

The following is how to define the metric and fluid variables in the `"diffgeo.m"` language.

```
In[1]:= coord = {t, r, x, y};
        $Assumptions = And[t ∈ Reals, x ∈ Reals, y ∈ Reals, r > 0];
        metricsign = -1;
        metric = {{-f[r], 0, 0, 0}, {0, g[r], 0, 0}, {0, 0, 1/r^2, 0},
           {0, 0, 0, 1/r^2}};
        vA = {h[r], 0, 0, 0}
        vF = partial[vA] - transpose[partial[vA], {2, 1}]

In[13]:= u = {√f[r], 0, 0, 0};
         vT = (p[r] + ρ[r]) u ** u + (p[r] metric);
         vJ = σ[r] u;
```

Note that all matrixes and arrays in this package have lower indices. The fluid variables are all written without a hat for simplicity. The Maxwell equation can be simplified as

```
In[16]:= eqnF = Simplify[contract[covariant[vF], {1, 2}] - vJ ]
```

$$\text{Out[16]=}\ \left\{-\sqrt{f[r]}\ \sigma[r] + \frac{\left(-\frac{2}{r} - \frac{f'[r]}{2f[r]} - \frac{g'[r]}{2g[r]}\right) h'[r] + h''[r]}{g[r]}, 0, 0, 0\right\}$$

By setting the first component of `eqnF` to be zero, we obtain the first equation of motion. The next equation of motion is the conserved current which can be derived from the Bianchi identity. This equation indicates that the gradient of the energy-momentum tensor in the presence of the 2-form field strength F^{AB} has the following form

$$\nabla_A T^{AB} = g_{CD} J^C F^{DB} \tag{C.5}$$

The input and output in the mathematica should look like

```
In[16]:= contract[covariant[vT], {1, 2}] - contract[vJ ** vF, {1, 2}]
```

$$\text{Out[16]=}\ \left\{0, \frac{(p[r] + \rho[r])\, f'[r]}{2f[r]} - \frac{\sigma[r]\, h'[r]}{\sqrt{f[r]}} + p'[r], 0, 0\right\}$$

The simplest term, {r,r}=0, will be the second equation of motion. Lastly, one can substitute the fluid variables and the metric ansatz (C.4) into the Einstein field equation. The (LHS)-(RHS) of the equation (C.1) are presented below

```
In[42]:= eqnR = Simplify[RicciTensor - metric RicciScalar/2 - 3 metric -
            (contract[vF ** vF, {2, 4}] - metric/4 (contract[vF ** vF, {1, 3}, {2, 4}])) - vT]
```

Out[43]=

{t, t}	$-\frac{2f[r]\left(5g[r]+r^2 g[r]^2(-3+\rho[r])+r\,g'[r]\right)+r^2 g[r]\,h'[r]^2}{2r^2 g[r]^2}$
{r, r}	$-g[r]\,(3+p[r]) + \frac{2f[r]-2r\,f'[r]+r^2 h'[r]^2}{2r^2 f[r]}$
{x, x} {y, y}	$-\frac{1}{4r^4 f[r]^2 g[r]^2}\left(r^2 g[r]\,f'[r]^2 + 2f[r]^2\left(-4g[r]+2r^2 g[r]^2(3+p[r]) - r\,g'[r]\right) + r\,f[r]\left(r\,f'[r]\,g'[r] + 2g[r]\left(f'[r] + r\,h'[r]^2 - r\,f''[r]\right)\right)\right)$

We pick the {r,r} component as the third equation. One should see that the other expressions which should be equal to zero seem to be very complicated. However, we can combine the {t,t} and {r,r} components and obtain the last equation

```
In[45]:= Simplify[((eqnR[[1]][[1]] * g[r] ^ 2) + (eqnR[[2]][[2]] * f[r] * g[r])) / f[r]]

Out[45]= (-r g[r] f'[r] + f[r] (-4 g[r] + r^2 g[r]^2 (p[r] + ρ[r]) - r g'[r])) / (r^2 f[r])
```

To sum up, the equations of motions of in terms of the fluid variables written in the same order as we obtained from the above calculation are

$$h'\left(-\frac{f'}{2f}-\frac{g'}{2g}-\frac{2}{r}\right)+h''-\sqrt{f}g\hat{\sigma} = 0\,; \tag{C.6}$$

$$\hat{p}'+\frac{(\hat{p}+\hat{\rho})f'}{2f}-\frac{\hat{\sigma}h'}{\sqrt{f}} = 0\,; \tag{C.7}$$

$$\frac{f'}{rf}-\frac{h'^2}{2f}+(3+\hat{p})g-\frac{1}{r^2} = 0\,; \tag{C.8}$$

$$\frac{1}{r}\left(\frac{f'}{f}+\frac{g'}{g}+\frac{4}{r}\right)+(\hat{p}+\hat{\rho})g = 0\,. \tag{C.9}$$

One can show that the complicated expressions in `eqnR` are identically zero once these four equations satisfied. These equations are the one that appears in [85]. The details about solving these equations can be found in [85, 88]

Bibliography

[1] 2012. URL https://www.simonsfoundation.org/quanta/20130701-signs-of-a-stranger-deeper-side-to-natures-building-blocks/.

[2] J. Zaanen, Y.-W. Sun, Y. Liu, and K. Schalm. The AdS/CMT guide for plumbers and electricians. *to be appear*, 2013.

[3] Angel M. Uranga. *Introduction to String Theory*, 2005. URL http://members.ift.uam-csic.es/auranga/Lect.pdf.

[4] J. Polchinski. *String Theory*. CUP, 2005.

[5] D. Tong. *Lectures on String Theory*, 2009. URL http://arxiv.org/abs/0908.0333.

[6] B. Zwiebach. *A First Course In String Theory*. CUP, 2009.

[7] J. McGreevy. 8.821 String Theory, Fall 2008. *MIT OpenCourseWare: Massachusetts Institute of Technology*, 2008. URL http://ocw.mit.edu/courses/physics/8-821-string-theory-fall-2008.

[8] O. Aharony, S. S. Gubser, J. M Maldacena, H. Ooguri, and Y. Oz. Large n field theories, string theory and gravity. *Phys.Rept.*, 323:183–386, 2000. URL arxiv.org/abs/hep-th/9905111.

[9] E. D'Hoker and D. Z. Freedman. Supersymmetric Gauge Theories and the AdS/CFT. *Lecture notes at TASI 2001 : Strings, Branes and Extra Dimensions*, 2001. URL http://arxiv.org/abs/hep-th/0201253.

[10] P. Di Francesco, P. Mathieu, and D. Senechal. *Conformal Field Theory*. Springer, 1997.

[11] E. Kiritsis. *String Theory in a Nutshell*. Princeton University Press, 2007.

[12] A. Zee. *Einstein Gravity in A Nutshell*. Princeton University Press, 2013.

[13] J. M. Maldacena. The Large N limit of superconformal field theories and supergravity. *Adv.Theor.Math.Phys.*, 2:231–252, 1998. URL http://arxiv.org/abs/hep-th/9711200.

[14] P. K. Kovtun, D. T. Son, and A. O. Starinets. Viscosity in strongly interacting quantum field theories from black hole physics. *Phys.Rev.Lett.*, 94:111601, 2005.

[15] J. Zaanen. A modern, but way too short history of the theory of superconductivity at a high temperature. In H. Rochalla and P. H. Kes, editors, *100 years of superconductivity*. Taylor & Francis Books, 2012. URL http://arxiv.org/abs/1012.5461.

[16] Pierre Coleman. *Introduction to Many Body Physics*, 2012. URL http://www.physics.rutgers.edu/~coleman/mbody/pdf/bk.pdf.

[17] S. Sachdev. The quantum phases of matter. *Rapporteur presentation at the 25th Solvay Conference on Physics, "The Theory of the Quantum World", Brussels,*, 2012. URL http://arxiv.org/abs/1203.4565.

[18] P. Nozieres and D. Pines. *The Theory of Quantum Liquid*. Perseus Book, 1999.

[19] J. Polchinski. Effective Field Theory and the Fermi Surface. *TASI lecture 1992*, 1992. URL http://arxiv.org/abs/hep-th/9210046.

[20] R. Shankar. Renormalization Group Approach to Interacting Fermions. *Rev. Mod. Phys*, 66:129–192, 1994. URL http://arxiv.org/abs/cond-mat/9307009.

[21] N. Iqbal, H. Liu, and M. Mezei. Lectures on holographic non-fermi liquids and quantum phase transitions. *TASI lecture 2010*, 2011. URL http://arxiv.org/abs/1110.3814v1.

[22] D. K. K. Lee and A. J. Schofield. Metals without electrons : the physics of exotic quantum fluid. In J. M. T. Thompson, editor, *Visions of the future : Physics and Electronics*. CUP, 2001.

[23] A. J. Leggett. *Quantum Liquid : Bose-Einstein condensation and Cooper pairing in condensed matter system*. OUP, 2006.

[24] Albert Furrer. Neutron scattering investigations of charge inhomogeneities and the pseudogap state in high-temperature superconductors. In K.Alex Müller and Annette Bussmann-Holder, editors, *Superconductivity in Complex Systems*, volume 114 of *Structure and Bonding*, pages 171–204. Springer Berlin Heidelberg, 2005. ISBN 978-3-540-23124-0. URL http://dx.doi.org/10.1007/b101020.

[25] J. Zaanen, F. Kruger, J.-H. She, D. Sadri, and S. I. Mukhin. Pacifying the fermi-liquid: battling the devious fermion signs. 2008. URL http://arxiv.org/abs/0802.2455.

[26] R. P. Feynman. *Statistical Mechanics, A Set of Lectures*. Benjamin/Cummings, 1982.

[27] M.A. Nielsen and I.L. Chuang. *Quantum Computation and Quantum Information*. CUP, 2000.

[28] E.Abraham and C.M. Varma. What angle-resolved photoemission experiments tell about the microscopic theory for high-temperature superconductors. *PNAS*, 97:5714, 2000.

[29] C. M. Varma, P. B. Littlewood, S. Scmitt-Rink, E. Abrahams, and A. E. Ruckenstein. Phenomenological of the normal state of cu-o high temperature superconductors. *Phys. Rev. Lett.*, 63:1996–1999, 1989.

[30] S. A. Hartnoll. Lectures on holographic methods for condensed matter physics. *Class.Quant.Grav.*, 26(22402), 2009. URL http://arxiv.org/abs/0903.3246.

[31] S. Sachdev. *Quantum Phase Transition*. CUP, 1999.

[32] L. Balents. Spin liquids in frustrated magnets. *Nature*, 464:199–208, 2010.

[33] S. Sachdev. What can gauge-gravity duality teach us about condensed matter physics? *Annual Review of Condensed Matter Physics*, 3(9), 2012. URL http://arxiv.org/abs/1108.1197.

[34] S. Sachdev and M. Műller. Quantum criticality and black holes. *J. Phys.: Condens. Matter*, 21(164216), 2009. URL http://arxiv.org/pdf/0810.3005v1.pdf.

[35] 2012. URL http://qpt.physics.harvard.edu/talks/imperial12.pdf.

[36] T. Grover, Y. Zhang, and A. Vishwanath. Entanglement entropy as a portal to the physics of quantum spin liquids. *New Journal of Physics*, 15:025002, 2013. URL http://arxiv.org/abs/1302.0899.

[37] S. Ryu and T. Takayanagi. Aspects of holographic entanglement entropy. *JHEP*, 0608: 045, 2006. URL http://arxiv.org/abs/hep-th/0605073.

[38] 2013. URL http://qpt.physics.harvard.edu/simons/Swingle.pdf.

[39] S. A. Hartnoll, P. K. Kovtun, M. Műller, and S. Sachdev. Theory of the nernst effect near quantum phase transitions in condensed matter, and in dyonic black holes. *Phys. Rev. B*, 76:144502, 2007. URL http://arxiv.org/abs/0706.3215.

[40] K. Becker, M. Becker, and J. H. Schwarz. *String Theory and M-Theory*. CUP, 2007.

[41] F. Denef and S. A. Hartnoll. Landscape of superconducting membranes. *Phys. Rev. D*, 79:126008, 2009. URL http://arxiv.org/abs/0901.1160.

[42] J. Gauntlett, J. Sonner, and T. Wiseman. Holographic superconductivity in m-theory. *Phys. Rev. Lett.*, 103:151601, 2009. URL http://arxiv.org/abs/0907.3796.

[43] S. S. Gubser, C. P. Herzog, S. S. Pufu, and T. Tesileanu. Superconductors form superstrings. *Phys. Rev. Lett.*, 103:141601, 2009. URL http://arxiv.org/abs/0907.3510.

[44] J. Gauntlett, J. Sonner, and D. Waldram. Universal fermionic spectral functions from string theory. *Phys. Rev. Lett.*, 107:241601, 2011. URL http://arxiv.org/abs/1106.4694.

[45] O. DeWolfe, S. S. Gubser, and C. Rosen. Fermi surfaces in maximal guaged supergravity. *Phys. Rev. Lett.*, 108:251601, 2011. URL http://arxiv.org/abs/1112.3036.

[46] O. Bergman, N. Jokela, G. Lifschytz, and M. Lippert. Quantum hall effect in a holographic model. *JHEP*, 1010:063, 2010. URL http://arxiv.org/abs/1003.4965.

[47] H. Ooguri and C.-S. Park. Holographic end-point of spatially modulated phase transition. *Phys. Rev. D*, 82:126001, 2010. URL http://arxiv.org/abs/1007.3737.

[48] A. Donos and J. Gauntlett. Holographic striped phases. *JHEP*, 1008:140, 2011. URL http://arxiv.org/abs/1106.2004.

[49] J. Erdmenger, N. Evans, I. Krisch, and E. Threlfall. Mesons in gauge/gravity duals - a review. *Eur.Phys.J.A*, 35:81–133, 2008. URL http://arxiv.org/abs/arXiv:0711.4467.

[50] J. McGreevy. Holographic duality with a view toward many-body physics. *Adv.High Energy Phys.*, 2010(723105), 2009. URL http://arxiv.org/abs/0909.0518.

[51] I. Heemskerk and J. Polchinski. Holographic and wilsonian renormalization groups. *JHEP*, 06(9):031, 2011. URL http://arxiv.org/abs/1010.1264.

[52] S. A. Hartnoll. Horizons, holography and condensed matter. In G. Horowitz, editor, *Black Holes in Higher Dimensions*. CUP, 2011. URL http://arxiv.org/abs/1106.4324.

[53] N. Iqbal and H. Liu. Real-time response in ads/cft with application to spinors. *Fortsch.Phys.*, 57:367–384, 2009. URL http://arxiv.org/abs/0903.2596.

[54] D. Tong and J. A. Laia. Flowing between fermionic fixed points. *JHEP*, 11:131, 2011. URL http://arxiv.org/abs/1108.2216.

[55] V. Balasubramanian and P. Kraus. A strss tensor for Anto-de Sitter gravity. *Commum. Math. Phys.*, 208:413–428, 1999. URL http://arxiv.org/abs/hep-th/9902121.

[56] K. Skenderis. Lecture notes on holographic renormalization. *Class.Quant.Grav.*, 19:5849–5876, 2002. URL http://arxiv.org/abs/hep-th/0209067.

[57] P. M. Chaikin and T. C. Lubensky. *Principle of condensed matter physics*. CUP, 1995.

[58] A. Altland and B. D. Simons. *Condensed Matter Field Theory*. CUP, 2nd edition, 2010.

[59] A. Strominger and C. Vafa. Microscopic origin of the bekenstein-hawking entropy. *Phys. Lett. B.*, 379:99–104, 1996. URL http://arxiv.org/abs/hep-th/9601029.

[60] S. A. Hartnoll and L. Huijse. Fractionalization of holographic fermi surface. *Class. Quant. Grav.*, 29:194001, 2012. URL http://arxiv.org/abs/1111.2606.

[61] N. Iqbal, H. Liu, and M. Mezei. Semi-local quantum liquids. *JHEP*, 04:086, 2011. URL http://arxiv.org/abs/1105.4621.

[62] T. Faulkner, H. Liu, J. McGreevy, and D. Vegh. Emergent quantum criticality, fermi surfaces, and AdS2. *Phys. Rev. D*, 83:125002, 2011. URL http://arxiv.org/abs/0907.2694.

[63] S. S. Gubser. Breaking an abelian gauge symmetry near a black hole horizon. *Phys. Rev. D.*, 78:065034, 2008. URL http://arxiv.org/abs/0801.2977.

[64] S. A. Hartnoll, C. P. Herzog, and G. T. Horowitz. Building an ads/cft superconductor. *Phys. Rev. D.*, 101:031601, 2008. URL http://arxiv.org/abs/0803.3295.

[65] S. A. Hartnoll, C. P. Herzog, and G. T. Horowitz. Holographic superconductors. *JHEP*, 0812:015, 2008. URL http://arxiv.org/abs/0810.1563.

[66] S.-S. Lee. A non-fermi liquid from a charged black hole; a critical fermi ball. *Phys. Rev. D*, 79:086006, 2009. URL http://arxiv.org/abs/0809.3402.

[67] H. Liu, J. McGreevy, and D. Vegh. Non-fermi liquids from holography. *Phys. Rev. D*, 83:065029, 2011. URL http://arxiv.org/abs/arXiv:0903.2477.

[68] M. Cubrovic, J. Zaanen, and K. Schalm. String theory, quantum phase transitions and the emergent fermi-liquid. *Science*, 325:439–444, 2009. URL http://arxiv.org/abs/0904.1993.

[69] Z. Q. Li, E. A. Henriksen, Z. Jiang, Z. Hao, M.C. Martin, P. Kim, H. L. Stormer, and D. N. Basov. Dirac charge dynamics in graphene by infrared spectroscopy. *Nature Physics*, 4:532–535, 2008. URL http://www.nature.com/nphys/journal/v4/n7/full/nphys989.html.

[70] G. T. Horowitz, J. E. Santos, and D. Tong. Optical conductivity with holographic lattices. *JHEP*, 07:168, 2012. URL http://arxiv.org/abs/1204.0519.

[71] G. T. Horowitz, J. E. Santos, and D. Tong. Further evidence for lattice-induced scaling. *JHEP*, 11:102, 2012. URL http://arxiv.org/abs/1204.0519.

[72] D. Vegh. Holography without translational symmetry. January 2013. URL http://arxiv.org/abs/1301.0537.

[73] R. A. Davison. Momentum relaxation in holographic massive gravity, 2013. URL http://arxiv.org/abs/1306.5792.

[74] S. W. Hawking and D. N. Page. Thermodynamics of black holes in Anti-De Sitter space. *Commum. Math. Phys.*, 87:577, 1983.

[75] E. Witten. Anti-de sitter space, thermal phase transition, and confinement in gauge theories. *Adv. Theor. Math. Phys.*, 2:505–532, 1998. URL http://arxiv.org/abs/hep-th/9803131.

[76] A. Zee. *Quantum Field Theory In A Nutshell*. Princeton University Press, 2nd edition, 2010.

[77] S. A. Hartnoll and D. Radicevic. Holographic order parameter for charge fractionalization. *Phys. Rev. D*, 86:066001, 2012. URL http://arxiv.org/abs/1205.5291.

[78] T. Nishioka, S. Ryu, and T. Takayanagi. Holographic entanglement entropy: An overview. *J. Phys. A*, 42:504008, 2009. URL http://arxiv.org/abs/0905.0932.

[79] L. Huijse and S. Sachdev. Fermi surfaces and gauge-gravity duality. *Phys. Rev. D*, 84:026001, 2011. URL http://arxiv.org/abs/1104.5022.

[80] B. Pioline and J. Troost. Schwinger pair production in ads2. *JHEP*, 0503:043, 2005. URL http://arxiv.org/abs/hep-th/0501169.

[81] L. Huijse, S. Sachdev, and B. Swingle. Hidden fermi surfaces in compressible states of gauge-gravity duality. *Phys. Rev. B*, 85:035121, 2012. URL http://arxiv.org/abs/1112.0573.

[82] T. Faulkner, N. Iqbal, H. Liu, J. McGreevy, and D. Vegh. http://arxiv.org/pdf/1003.1728v1.pdf, 2010. URL http://arxiv.org/pdf/1003.1728v1.pdf.

[83] M. Cubrovic, J. Zaanen, and K. Schalm. Constructing the AdS dual of a fermi liquid: AdS black holes with Dirac hair. *JHEP*, 1110:017, 2011. URL http://arxiv.org/abs/1012.5681.

[84] M. V. Medvedyeva, E. Gubankova, M. Cubrovic, K. Schalm, and J. Zaanen. Quantum corrected phase diagram of holographic fermions, 2013. URL http://arxiv.org/abs/1302.5149.

[85] S. A. Hartnoll and A. Tavanfar. Electron stars for holographic metallic criticality. *Phys. Rev. D*, 83:046003, 2011. URL http://arxiv.org/abs/1008.2828.

[86] S. A. Hartnoll, D. M. Hofman, and A. Tavanfar. Holographically smeared fermi surface: Quantum oscillations and Luttinger count in electron stars. *Europhys. Lett.*, 95:31002, 2011. URL http://arxiv.org/abs/1011.2502.

[87] S. A. Hartnoll, D. M. Hofman, and D. Vegh. Stellar spectroscopy: Fermions and holographic lifshitz criticality. *JHEP*, 1008:096, 2011. URL http://arxiv.org/abs/1105.3197.

[88] S. A. Hartnoll, J. Polchinski, E. Silverstein, and D. Tong. Towards strange metallic holography. *JHEP*, 1004:120, 2010. URL http://arxiv.org/abs/0912.1061.

[89] S. Kachru, X. Liu, and M. Mulligan. Gravity duals of lifshitz-like fixed points. *Phys. Rev. D*, 78:106005, 2008. URL http://arxiv.org/abs/0808.1725v2.

[90] J. de Boer, K. Papadodimas, and E. Verlinde. Holographic neutron stars. *JHEP*, 10:020, 2010. URL http://arxiv.org/abs/0907.2695.

[91] S. A. Hartnoll and P. Petrov. Electron star birth: A continuous phase transition at nonzero density. *Phys. Rev. Lett.*, 106:121601, 2011. URL http://arxiv.org/abs/1011.6469.

[92] C. Charmousis, B. Goutéraux, B. S. Kim, E. Kiritsis, and R. Meyer. Effective holographic theories for low-temperature condensed matter systems. *JHEP*, 11:151, 2010.

[93] X. Dong, S. Harrison, S. Kachru, G. Torroba, and H. Wang. Aspects of holography for theories with hyperscaling violation. *JHEP*, 1206:041, 2012. URL http://arxiv.org/abs/1201.1905.

[94] N. Iizaku, N. Kundu, P. Narayan, and S. Trivedi. Holographic fermi and non-fermi liquids with transitions in dilaton gravity. *JHEP*, 01:094, 2012. URL http://arxiv.org/abs/1105.1162.

[95] J. Erlich, E. Katz, D. T. Son, and M. A. Stephanov. Qcd and a holographic model of hadrons. *Phys. Rev. Lett.*, 95:261602, 2005. URL http://arxiv.org/abs/hep-ph/0501128.

[96] A. Karch, E. Katz, D. T. Son, and M. A. Stephanov. Linear confinement and AdS/QCD. *Phys. Rev. D*, 74:015005, 2006. URL http://arxiv.org/abs/hep-ph/0602229.

[97] G. T. Horowitz and B. Way. Complete phase diagrams for a holographic superconductor/insulator system. *JHEP*, 11:011, 2010. URL http://arxiv.org/abs/1007.3714.

[98] T. Nishioka, S. Ryu, and T. Takayanagi. Holographic superconductor/insulator transition at zero temperature. *JHEP*, 03:131, 2010. URL http://arxiv.org/abs/0911.0962.

[99] S. Sachdev. A model of a fermi liquid using gauge-gravity duality. *Phys. Rev. D*, 84 (066009), 2011. URL http://arxiv.org/abs/1107.5321.

[100] A. Allais, J. McGreevy, and J. Suh. A quantum electon star. *Phys. Rev. Lett.*, 108:231602, 2012. URL http://arxiv.org/abs/1202.5308.

[101] A. Allais and J. McGreevy. How to construct a gravitating quantum electron sta. URL http://arxiv.org/abs/1306.6075.

[102] J. Bhattacharya, N. Ogawa, T. Takayanagi, and T. Ugajin. Soliton stars as holographic confined fermi liquids. *JHEP*, 02:137, 2012. URL http://arxiv.org/abs/1201.0764.

[103] M. Blake, S. Bologesi, D. Tong, and K. Wong. Holographic dual of the lowest landau level. *JHEP*, 1212:039, 2012. URL http://arxiv.org/abs/1208.5771.

[104] S. Sachdev. URL http://qpt.physics.harvard.edu/talks/kitp11.pdf.

[105] S. Sachdev. The landscape of the Hubbard model. *TASI and Chandrasekhar lecture 2010*, 2010. URL http://arxiv.org/abs/1012.0299.

[106] T. Senthil, S. Sachdev, and M. Vojta. Quantum phase transitions out of the heavy fermi liquid. *Physica B*, 9:359–361, 2005. URL http://arxiv.org/abs/cond-mat/0409033.

[107] F. Nitti, G. Policastro, and T. Vanel. Dressing the electron star in a holographic superconductor, 2013. URL http://arxiv.org/abs/1307.4558.

[108] Y. Liu, K. Schalm, Y.-W. Sun, and J. Zaanen. Bose-fermi competition in holographic metals, 2013. URL http://arxiv.org/abs/1307.4572.

[109] M. Nozaki, T. Numasawa, and T. Takayanagi. Holographic local quenches and entanglement density. *JHEP*, 1305:080, 2013. URL http://arxiv.org/abs/1302.5703.

[110] C. Nayak, S. H. Simon, A. Stern, M. Freedman, and S. Das Sarma. Non-abelian anyons and topological quantum computation. *Rev. Mod. Phys*, 80:1083, 2008. URL http://arxiv.org/abs/0707.1889.

[111] A. Kitaev and J. Preskill. Topological entanglement entropy. *Phys. Rev. Lett.*, 96:110404, 2006. URL http://arxiv.org/abs/hep-th/0510092.

[112] Hui Li and F. D. M. Haldane. Entanglement spectrum as a generalization of entanglement entropy: Identification of topological order in non-abelian fractional quantum hall effect states. *Phys. Rev. Lett.*, 101:010504, 2008. URL http://arxiv.org/abs/0805.0332v2.

[113] J. L. Davis, P. Kraus, and A. Shah. Gravity dual of a quantum hall plateau transition. *JHEP*, 0811:020, 2008.

[114] S. Ryu and T. Takayanagi. Topological insulators and superconductors from string theory. *Phys. Rev. D*, 82:086014, 2010. URL http://arxiv.org/abs/1007.4234.

[115] C. Kristjansen and G. W. Semenoff. Giant d5 brane holographic hall state. *JHEP*, 1306: 048, 2013. URL http://arxiv.org/abs/1212.5609.